

Global Model of the General Circulation Of the Atmosphere Below 75 Kilometers With an Annual Heating Cycle

KEVIN E. TRENBERTH¹—*Department of Meteorology, Massachusetts Institute of Technology, Cambridge, Mass.*

ABSTRACT—The development of a nine-layer, quasi-geostrophic, highly truncated spectral model of the atmosphere is described. The model is global, extends to 0.05 mb (71 km) with roughly 10-km resolution in the stratosphere, and includes an annual heating cycle. Preliminary integrations without eddies reveal the seasonal variation of a thermally driven circulation.

A model integration was made to simulate the months of December and January without nonzonal forcing, thus being more representative of a Southern Hemisphere winter. The overall features of the atmosphere were well simulated. A midlatitude temperature maximum was

produced in the winter mesosphere of the model, which was driven in the manner of the lower stratosphere. With the inclusion of the annual heating cycle, the model successfully reproduced a more intense circulation in January than existed in December. This caused the maximum tropospheric meridional temperature gradient in the winter hemisphere to occur weeks prior to the maximum in the external heating field. A seasonally coupled index cycle in the very long waves was of significance in producing transient upward energy propagation and, as such, may be the source of sudden stratospheric warming events.

CONTENTS

1. Introduction.....	287
2. Model formulation.....	288
a. Requirements.....	288
b. Energy source and sink representation.....	288
c. Boundary conditions.....	289
d. Method of solution.....	289
e. Numerical values of parameters.....	291
f. Annual heating cycle.....	292
3. Model energetics.....	292
4. Preliminary solutions.....	293
a. Symmetric integration.....	293
b. Baroclinic growth rates.....	293
c. Introduction of eddies.....	295
5. Results of experiment A: no nonzonal forcing.....	296
a. Zonally averaged fields.....	296
b. Energy budget.....	298
c. The mesosphere in winter.....	301
d. Angular momentum budget.....	301
e. Source of discrepancies.....	302
6. Effects of annual heating cycle.....	302
7. Concluding remarks.....	303
Appendix.....	304
Acknowledgments.....	304
References.....	304

1. INTRODUCTION

In recent years, the sudden stratospheric warming phenomenon has been the subject of many investigations, but the causes and mechanisms of the event are still not fully understood. Studies of the general circulation of the stratosphere have been limited in the past by the number of observations, especially above 10 mb, and very few attempts have been made to model the region. Energetics

studies of the lower stratosphere have revealed the importance of the vertical flux of eddy geopotential energy out of the troposphere into this region (e.g., Oort 1964a). Reed et al. (1963), Muench (1965), Julian and Labitzke (1965), and others have shown the importance of this long-wave energy flux into the region where a sudden stratospheric warming is occurring.

This study is concerned with tropospheric-stratospheric coupling and the events associated with it. Thus, a number of hypotheses were established at the outset with regard to the various processes that may lead to a sustained increased flux of long-wave energy into the stratosphere and thereby perhaps to a sudden warming (Trenberth 1973). To test these hypotheses, we constructed a numerical model of the atmosphere.

Clearly, such a model must be extensive in the vertical. Of the few previous attempts to model the stratosphere, Byron-Scott (1967) used a simple three-layer model based on the Burger (1958) diagnostic quasi-geostrophic equations to predict the events in a stratospheric layer bounded above and forced from below. The experiment revealed the importance of abrupt changes in the forcing of the region. A similar conclusion could be drawn from the results of a six-level, quasi-geostrophic spectral model developed by Clark (1970). However, this model had a serious deficiency: it did not conserve angular momentum because of an incorrect formulation of frictional dissipation. The most sophisticated stratospheric model has been that of Manabe and Hunt (1968). Using an 18-level primitive-equation model, they were able to reproduce well-defined features in the lower stratosphere, and they found that the vertical eddy energy flux may extend to high altitudes.

¹ Now affiliated with the New Zealand Meteorological Service, Wellington

The purpose of this paper is to describe the numerical model development and certain features revealed by the integrations. A second paper (Trenberth 1973) will describe the experiments and the results pertaining to the central theme of tropospheric-stratospheric interaction, as outlined above.

2. MODEL FORMULATION

a. Requirements

It is desirable to work with as simple a model as possible to obtain mathematical tractability and still include all the important features of the atmospheric phenomenon we wish to investigate. If we were to choose a full-scale primitive-equation model, reasons for the success or lack of success in attaining our goals might be difficult to determine (e.g., Miyakoda et al. 1970).

Lorenz (1960*b*) and Charney (1962) performed systematic derivations of simplified sets of equations from the primitive equations. The quasi-geostrophic approximation omits the transport of momentum by the vertical motions and by the divergent part of the wind. Hence, it omits the net transport of momentum by the mean meridional cell. However, these terms may reasonably be neglected in the present investigation. In addition, the quasi-geostrophic assumption is valid only if tidal motions have amplitudes less than that of the mean zonal wind; that is, below about 80 km (Hines 1963).

The thermodynamic equation may be simplified by allowing the static stability, σ , to vary as a function of pressure and time, or by also suppressing the temporal dependence (Bryan 1959, Lorenz 1960*b*, 1962). The additional nonlinear terms introduced in a multilevel model in the former case would increase computation time by roughly a factor of two. This feature [i.e., $\sigma = \sigma(p, t)$] proved to be of importance in Bryan's two-level model, but the effects are most likely less important in a multilevel model with a stratosphere. Therefore, we use $\sigma = \sigma(p)$, but with the knowledge that we shall be unable to simulate the increasing static stability with the onset of winter.

The p dependence will be removed by taking finite differences in the vertical. However, instead of representing the variables as discrete functions on a mesh, thereby including many scales of motion, we further simplified the model by representing variables as highly truncated spectral functions.

The advantages are: (1) mapping on a sphere is not necessary, thereby eliminating finite-difference difficulties at the pole; (2) the interaction coefficients between the retained modes are treated exactly so that energy is conserved in nonlinear interactions, and no instability due to aliasing errors can exist; and (3) each wave number may be easily isolated, and only those waves of interest need be included.

Lorenz (1960*a*) proposed the use of orthogonal function series expansions for each dependent variable after omitting certain physical features or processes believed to be of secondary importance. The series are then truncated, and all but a small number of functions are discarded. The

coefficients of the retained orthogonal functions become the new dependent variables, and the new equations are ordinary differential equations. The method is illustrated by Lorenz (1960*a*, 1962, 1963), Bryan (1959), Peng (1965), Clark (1970), and others.

Following Lorenz (1960*b*), one may write the energetically consistent set of equations with pressure, p , as the vertical coordinate as follows:

$$\frac{\partial}{\partial t} \nabla^2 \psi = -J(\psi, \nabla^2 \psi + f) + \nabla \cdot \left(f \nabla \frac{\partial \chi}{\partial p} \right) + \nabla \cdot \mathbf{F} \times \mathbf{k}, \quad (1)$$

$$\frac{\partial \theta}{\partial t} = -J(\psi, \theta) + \sigma \omega + \frac{Q}{c_p} \left(\frac{p_{00}}{p} \right)^\kappa, \quad (2)$$

and

$$\nabla \cdot \left(f \nabla \frac{\partial \psi}{\partial p} \right) = -R p^{\kappa-1} p_{00}^{-\kappa} \nabla^2 \theta \quad (3)$$

where

$$\sigma = -\frac{\partial \theta_s}{\partial p} = \text{static stability,}$$

$$\omega = \nabla^2 \chi = p \text{ velocity,}$$

$$\psi = \text{stream function,}$$

$$\frac{\partial \chi}{\partial p} = \text{velocity potential,}$$

$$t = \text{time,}$$

$$J = \text{Jacobian operator, } J(A, B) = \nabla A \cdot \nabla B \times \mathbf{k},$$

$$f = 2\Omega \sin \phi = \text{Coriolis parameter,}$$

$$\Omega = \text{angular velocity of earth,}$$

$$\phi = \text{latitude,}$$

$$c_p = \text{specific heat of air at constant pressure,}$$

$$\theta = \text{potential temperature,}$$

$$Q = \text{rate of radiative heating per unit mass of air,}$$

$$\mathbf{F} = \text{friction per unit mass of air,}$$

$$p_{00} = \text{reference pressure (1000 mb),}$$

$$R = \text{gas constant for air, and}$$

$$\kappa = R/c_p = 2/7.$$

Equations (1), (2), and (3) are the vorticity equation, the thermodynamic equation, and the thermal wind equation, respectively.

b. Energy Source and Sink Representation

For long-term integrations of the equations, friction and heating must be included. We are not here interested in these processes themselves, only in the effects they have on the motion, and, therefore, a crude parameterization may suffice. Also, the exact mechanisms are extremely complicated and not known, and simple parameterization provides for greater control and knowledge of the actual forcing of the model atmosphere.

Following Charney (1959), we take

$$\mathbf{F} = -g \mathbf{k} \cdot \frac{\partial \boldsymbol{\tau}}{\partial p} \quad (4)$$

where $\boldsymbol{\tau} = -\mu \rho g (\partial \mathbf{V} / \partial p)$ is the stress vector, \mathbf{V} is the velocity vector, g is gravity ($9.8 \text{ m}\cdot\text{s}^{-2}$), and μ is the vertical eddy-viscosity coefficient. That is, we assume the stress to be proportional to the vertical wind shear.

We are interested in baroclinically unstable and long, forced waves and their interaction. They must be capable

of transporting heat and momentum and must include barotropic effects. Waves will be introduced to provide these mechanisms, but severe truncation will eliminate the effects of very short waves. To allow for this, we included lateral eddy-viscosity diffusion and eddy-heat diffusion in a manner similar to that used by Phillips (1956).

Thus, the total friction representation becomes

$$\nabla \cdot \mathbf{F} \times \mathbf{k} = g^2 \frac{\partial}{\partial p} \left(\rho \mu \frac{\partial}{\partial p} \nabla^2 \psi \right) + E_v \left(\nabla^2 + \frac{2}{a^2} \right) \nabla^2 \psi \quad (5)$$

where the last term in eq (5) includes the effect of a spherical earth, and E_v is the lateral kinetic eddy-viscosity coefficient.

Thermal forcing is complicated by the fact that heating and cooling are both operating with different time constants in the stratosphere. Methods have been devised for treating ozone as an extra variable (Byron-Scott 1967, Clark 1970) but they will not be so used here. In this way, the computation will be simplified and complementary effects of ozone on events such as the sudden stratospheric warming will be eliminated.

Above 10 mb, photochemical effects become of major importance and the treatment of Leovy (1964) is used. This utilizes the Newtonian cooling approximation to represent infrared heating, principally in the 15- μm CO_2 band, and a linearization of the absorption of solar energy, chiefly by ozone. In this way, we may express the heating rate, Q , by a generalized Newtonian heating and cooling with a time constant h given by

$$Q = h(T^* - T) \quad (6a)$$

where T is temperature and T^* is an equilibrium temperature profile that is a function of pressure, latitude and longitude, and time. The time constant, h , is a function of pressure alone and includes the effect of the temperature-dependent ozone photochemistry and Newtonian cooling (Leovy 1964, Trenberth 1972).

This form of heating will be adequate for our purposes, but it is a gross oversimplification. The deficiency is probably greatest near the stratopause where nonlinear effects may be important.

At lower levels, the ozone photochemistry may be ignored and this formulation should serve well, but latent heating, boundary-layer heating, and radiation should be included (Peng 1965).

With the addition of eddy-heat diffusion, the heating representation in eq (2) becomes

$$\frac{Q}{c_p} \left(\frac{p_{00}}{p} \right)^k = h(\theta^* - \theta) + E_T \nabla^2 \theta \quad (6b)$$

where E_T is the lateral eddy-diffusion coefficient for heat.

c. Boundary Conditions

The lower boundary condition will be $\omega=0$ at $p=p_{00}$ except when orography is introduced. Since we shall be using a limited number of spherical harmonics to represent

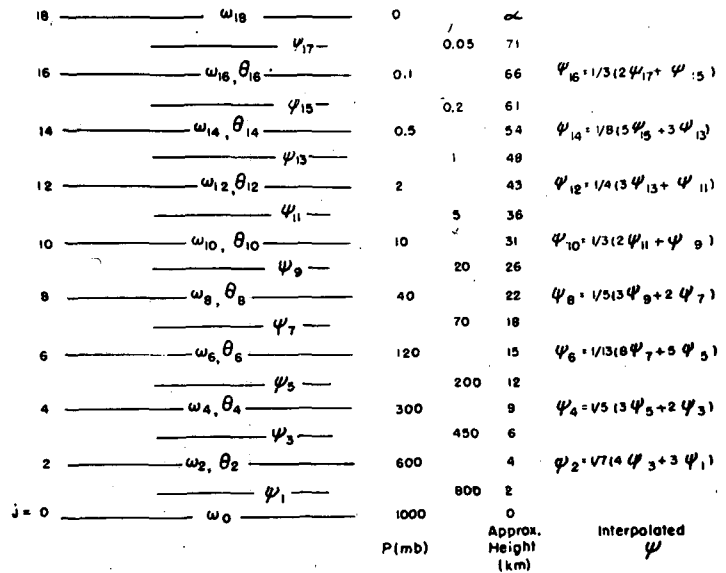


FIGURE 1.—Vertical resolution of the model.

the variables, we will be unable to include a realistic orography representation. Instead, we shall represent only the very large-scale orography in the Northern Hemisphere (N.H.) as best we can, while allowing completely spurious but relatively small features in the Southern Hemisphere (S.H.). We shall use the approximation

$$\omega = -\rho_0 g w = -\rho_0 g J(\psi, H) \quad (7)$$

where ρ_0 is a constant value of the air density and H is the mountain height profile, which will apply at the lower boundary. The upper boundary condition used is $\omega=0$ at $p=0$.

d. Method of Solution

Following Lorenz (1960b), we subdivided the model into n layers by the $n+1$ surfaces p_0, p_2, \dots, p_{2n} numbered from the ground upward. Unequal layers of p are chosen to emphasize the stratosphere (fig. 1). The system of differential equations is replaced by a system in which finite differences replace derivatives with respect to p in such a way that reversible adiabatic processes have equal effects on kinetic and potential energies. These equations are

$$\begin{aligned} \frac{\partial}{\partial t} \nabla^2 \psi_j = & -J(\psi_j, \nabla^2 \psi_j + f) + \frac{\nabla \cdot f \nabla (\chi_{j-1} - \chi_{j+1})}{p_{j-1} - p_{j+1}} \\ & - k_j \nabla^2 (\psi_j - \psi_{j-2}) - k'_j \nabla^2 (\psi_j - \psi_{j+2}) \\ & + E_v \left(\nabla^2 + \frac{2}{a^2} \right) \nabla^2 \psi_j, \quad (j=1, 3, \dots, 17) \end{aligned} \quad (8a)$$

where

$$k_j = \frac{\mu_{j-1} g^2 p_{j-1}}{RT_{j-1} (p_{j-2} - p_j) (p_{j-1} - p_{j+1})}, \quad (8b)$$

$$k'_j = \frac{\mu_{j+1} g^2 p_{j+1}}{RT_{j+1} (p_j - p_{j+2}) (p_{j-1} - p_{j+1})}, \quad (8c)$$

and $\psi_{-1}, \psi_{19}, k'_{17}$ are identically zero;

$$\frac{\partial \theta_j}{\partial t} = -J(\psi_j, \theta_j) + \sigma_j \nabla^2 \chi_j + h_j (\theta_j^* - \theta_j) + E_T \nabla^2 \theta_j, \quad (j=2, 4, \dots, 16) \quad (9)$$

$$R p_{00}^* p_j^{*-1} (p_{j-1} - p_{j+1}) \nabla^2 \theta_j = -\nabla \cdot f \nabla (\psi_{j-1} - \psi_{j+1}), \quad (j=2, 4, \dots, 16) \quad (10)$$

Using eq (7), we put

$$\nabla \cdot f \nabla \chi_0 = f_0 \nabla^2 \chi_0 = -f_0 \rho_0 g J(\psi_1, H). \quad (11)$$

This involves a further approximation since we shall choose a value of f_0 for midlatitudes of the N.H. This representation is adequate, however, since the orography in the S.H. is small and arbitrary in the model, and the effect is to shift the orography by one-half wave length.

This simple treatment has the advantage of conserving energy while distorting the flow to create eddy kinetic energy from the zonal form or vice versa. A more realistic formulation allowing for a variable f could be used, but, to conserve energy, one would have to define a temperature field at 1000 mb, thereby effectively changing the number of levels in the model.

For the above set of equations, we may readily make use of the concept of available potential energy. Therefore, in the absence of friction and diabatic heating, $A+K$ is conserved. Here, A and K are defined as

$$A = \frac{1}{2} R p_{00}^* \int p^{*-1} \sigma^{-1} (\bar{\theta} - \{\bar{\theta}\})^2 dM, \quad (12)$$

and

$$K = \frac{1}{2} \int \nabla \psi \cdot \nabla \psi dM, \quad (13)$$

where

$$dM = g^{-1} \sum_j (p_{j-1} - p_{j+1}) dS,$$

$\{\bar{\theta}\}$ is the mean over the domain, and dS is an element of horizontal area. We assume that the method of specifying χ_j (or ω_j) and θ_j for odd j , and ψ_j for even j is linear interpolation between levels (fig. 1).

We now expand $\nabla^2 \psi_j$, θ_j , and $\nabla^2 \chi_j$ from the closed set of eq (8)-(11), in the complete set of surface spherical harmonics,

$$\{Y_{|m|+l}^m; m=0, \pm 1, \pm 2, \dots; l=0, 1, 2, \dots\}, \quad (14)$$

where $Y_n^m = P_n^m e^{im\lambda}$ is the function of order m and degree n (or mode $n-m$). The order indicates the number of waves around a latitude circle and the mode indicates the number of zeros between the poles. P_n^m is the normalized associated Legendre function of order m and degree n .

When the complete set of expansions are obtained, we truncate to retain a finite number of terms, namely, the smallest subset capable of representing the features and mechanisms of interest and importance. Therefore, we choose to include only wave numbers 0, 2, 4, and 6. We expect waves 4 and 6 to play the role of baroclinically unstable waves with greatest growth rates while wave 2 belongs to the class of planetary waves and will be subjected to nonzonal forcing. The inclusion of all three waves will allow nontrivial interactions between waves to occur.

It is necessary to include Y_0^0 to represent a three-cell meridional circulation in each hemisphere. Hence, six modes are chosen to represent the zonal flow, but only three modes will be used to represent the eddies. We include asymmetric modes about the Equator, which requires careful handling of the heating field to ensure that an inflection point occurs at the Equator, and temperature gradients are small near there.

We expand as follows:

$$\nabla^2 \psi_j = \sum_{l=0,2,4,6} \zeta_{l,j}^0 Y_l^0 + \sum_{m=2,4,6} \sum_{l=1,2,3} (\zeta_{|m|+l,j}^m Y_{|m|+l}^m + \zeta_{|m|+l,j}^{-m} Y_{|m|+l}^{-m}), \quad (j=1, 3, \dots, 17) \quad (15)$$

$$\nabla^2 \chi_j = \sum_{l=0,2,4,6} \omega_{l,j}^0 Y_l^0 + \sum_{m=2,4,6} \sum_{l=0,1,2} (\omega_{|m|+l,j}^m Y_{|m|+l}^m + \omega_{|m|+l,j}^{-m} Y_{|m|+l}^{-m}), \quad (j=2, 4, \dots, 16) \quad (16)$$

and

$$\theta_j = \sum_{l=0,2,4,6} \theta_{l,j}^0 Y_l^0 + \sum_{m=2,4,6} \sum_{l=0,1,2} (\theta_{|m|+l,j}^m Y_{|m|+l}^m + \theta_{|m|+l,j}^{-m} Y_{|m|+l}^{-m}), \quad (j=2, 4, \dots, 16). \quad (17)$$

The coefficients are complex for $m \neq 0$ and we set

$$\zeta_{n,j}^{-m} = (-1)^m \bar{\zeta}_{n,j}^m,$$

$$\omega_{n,j}^{-m} = (-1)^m \bar{\omega}_{n,j}^m,$$

and

$$\theta_{n,j}^{-m} = (-1)^m \bar{\theta}_{n,j}^m,$$

where a bar indicates the complex conjugate. Then the expansions are real-valued.

Since nonlinear interactions, as well as terrestrial local vorticity, always disperse the spectra, the harmonics produced outside the prescribed finite spectra must be omitted to make the system of spectral equations closed and energetically self consistent. Therefore, eq (8)-(10) will be only approximately satisfied.

The resulting spectral equations are similar to those given by Peng (1965) and are presented in the appendix. We now have a system of simultaneous complex ordinary differential equations, which are solved by matrix inversion.

The finite-difference scheme used for the time integration was that proposed by Lorenz (1971), which provides for a multiple-order scheme where the number of steps required equals the order, N . Lorenz shows that $\Delta T/N$ may be considered as the fundamental time step and, provided it is short enough (less than about 1/17th of the period of the waves), the N -cycle scheme becomes increasingly accurate.

The computations were performed on an IBM 360/65 computer² at the Massachusetts Institute of Technology computation center. In the main integration, a fourth-order scheme was used and the largest time step for a stable scheme with sufficient accuracy was $\Delta T = 6$ hr ($\Delta T/N = 1.5$ hr). The real time taken to integrate the model for 1 day and perform subsidiary calculations was 22 s.

² Mention of a commercial product does not constitute an endorsement.

TABLE 1.—Values of parameters at pressure levels, p . T_0 is the mean global temperature for each layer. Other parameters are defined in text.

p	σ	T_0	μ	k	k'	E	h	θ_1^*	θ_2^*	θ_3^*
(mb)	(°/mb)	(°K)	(g·cm ⁻¹ ·s ⁻¹)	(10 ⁻⁷ s ⁻¹)	(10 ⁻⁷ s ⁻¹)	(m ² /s)	(10 ⁻⁶ s ⁻¹)			
1000	0.048		225							
800				20	10.7	10 ⁵				
600	.047	267	200			10 ⁴	0.926	7.57	-17.8	0
450				14.3	6.13	10 ⁵				
300	.14	236	108			10 ⁴	.680	8.42	-14.54	0
200				10.2	1.11	5×10 ⁴				
120	.8	209	13.5			10 ⁴	.222	16.42	-4.10	3.12
70				2.51	0.373	10 ⁴				
40	4.5	214	2.4			10 ³	.297	29.6	-11.65	8.34
20				0.995	.1036	10 ³				
10	34.	231	0.318			10 ²	.587	52.0	-20.1	17.02
5				.388	.0309	10 ²				
2	280.	263	.039			10	2.20	69.2	-31.7	32.2
1				.165	.0672	10				
0.5	880.	256	.0123			1	2.77	98.2	-15.6	42.9
0.2				.252	.032	1				
0.1	6400.	221	.0017			0	2.31	38.5	0	16.8
0.05				.128	0	0				

e. Numerical Values of Parameters

The parameters involved in the equations of the model are assigned values on the basis of previous experience of other authors with models and from observations of the real atmosphere. Models of the lower stratosphere and troposphere are abundant, as are observations, but data at higher levels are rare and somewhat uncertain. Models of the region are virtually nonexistent.

Values of θ_j representing January conditions in the N.H. were chosen from Murgatroyd (1970), and U.S. Standard Atmosphere Supplements (COESA 1966). Thus, a mean temperature was used to evaluate static stability and the k and k' terms. The static stability values were later modified slightly in the troposphere as described in subsection 4b.

Following Charney (1959) and Peng (1965), we let the coefficient of ground friction be $k_1=2\times 10^{-6}$ s⁻¹. The vertical eddy coefficient, μ , was assumed to be inversely proportional to the static stability, with $\mu_0=225$ g·cm⁻¹·s⁻¹ (Charney 1959). Thus, k and k' may be calculated.

The lateral eddy-viscosity coefficient and eddy-diffusion coefficient, E_v and E_T , are difficult to estimate. Peng (1965) chose $E_v=10^5$ m²/s and $E_T=0$. Phillips (1956) put $E_v=E_T=10^5$ m²/s. It seems E_T should be less than E_v , and probably both should decrease with height, since short waves are largely absent at higher levels.

Diabatic heating satisfies the equation

$$\frac{d\theta_j}{dt} = h_j(\theta_j^* - \theta_j).$$

Mean values of θ_j have been chosen. Below 10 mb, values of $d\theta_j/dt$ were taken from Newell et al. (1970) and include estimates of latent heat, boundary-layer heating, and radiative heating or cooling. Values of θ^* were estimated, principally using calculations by Manabe and Strickler (1964), with some adjustment at low levels as indicated

by Manabe and Möller (1961). A smoothed θ^* profile was chosen as best fit, using the first three modes. Thus, $\theta_4^* = \theta_5^* = \theta_6^* = 0$ at all levels. The values chosen represent solstice conditions and the annual heating cycle was incorporated as given in subsection 2f. Above 10 mb, a Newtonian cooling coefficient was estimated from Kuhn and London (1969) and Murgatroyd and Goody (1958), and the enhanced Newtonian coefficients h_j were found from the theory (Leovy 1964). Because of the non-linear nature of heating with temperature, θ^* is difficult to estimate, but with the aid of Murgatroyd (1970), Murgatroyd and Goody (1958), and Kuhn and London (1969), the values in table 1 were chosen. At 10 mb, both procedures were used and a compromise value was chosen. The enhanced Newtonian coefficients agree with those of Dickinson (1968).

The complete T^* field is presented in figure 2 and may be compared to the equilibrium field given by Murgatroyd (1970). The resemblance is strong at lower levels but differs considerably where photochemical damping plays an important role.

The major heating in the N.H. is caused by the land-sea contrast and is predominantly in wave 2. We shall consider only wave 2 nonzonal heating,

$$\theta_{n,j}^* = \theta_{n,j}^{*0} = 0.$$

The net asymmetric heating is not known, and difficulties in obtaining estimates are highlighted by Clapp (1961) who used two methods, the results of which were quite different. Katayama (1964) also presented estimates of tropospheric heating, which were used to evaluate the $\theta_{n,j}^{*2}$ for this study. The heating was arbitrarily distributed at the two tropospheric levels in the model in the ratio of 10:1 at 600 and 300 mb.

The latitudinal profile was chosen to produce small heating in the S.H. and small gradients at the Equator, so that the peak heating at 600 mb was 1.07°/day near 44°N,

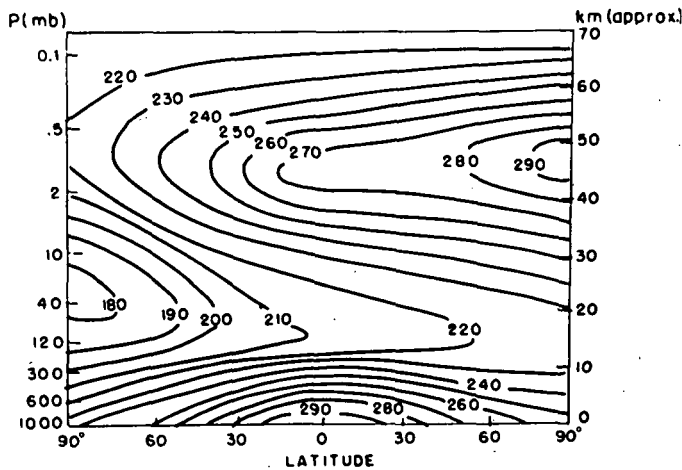


FIGURE 2.—The equilibrium temperature field, T^* , for the solstices.

TABLE 2.— θ_n^{*2} values (r =real part, i =imaginary part)

P (mb)	600 _r	600 _i	300 _r	300 _i
θ_2^{*2}	$2.17 \sin 2\gamma$	$-2.17 \cos 2\gamma$	$0.49 \sin 2\gamma$	$-0.49 \cos 2\gamma$
θ_3^{*2}	$2.73 \sin 2\gamma$	$-2.73 \cos 2\gamma$	$0.61 \sin 2\gamma$	$-0.61 \cos 2\gamma$
θ_4^{*2}	$4.17 \sin 2\gamma$	$-4.17 \cos 2\gamma$	$0.93 \sin 2\gamma$	$-0.93 \cos 2\gamma$

with a maximum in the S.H. of $0.4^\circ/\text{day}$ near 50°S . Using the h_r values found for the zonal heating, we chose the values given in table 2. A generalized phase angle γ is given here, where we used $\gamma=145^\circ$ (or -35°). These values were chosen to be representative values of the heating in wave 2. No attempt was made to represent the variation of phase with latitude or with height.

The phase of the mountains in wave 2 was chosen as 35°E . Therefore, peak warming will occur to the east of the mountains, and cooling to the west, which should produce an approximate in-phase reinforcement of the two effects. The exact relation will depend on the vertical structure of the wave.

Again using only wave 2, we select the latitudinal variation of H to have a peak in midlatitudes of the N.H., but smaller values in the S.H. and equatorial regions. The profile chosen was a peak of 1050 m (amplitude 525 m) near 45°N . A peak of 334 m (amplitude 167 m) then appears 90° out of phase near 30°S . Thus,

$$H = (210P_3^2 + 128P_4^2 + 63P_5^2) \sin 2(\lambda - 35^\circ)$$

which is substituted in eq (11).

f. Annual Heating Cycle

The heating function was considered with an annual heating cycle defined as follows. Heating components asymmetric about the Equator (θ_1^* , θ_3^*) were made to vary sinusoidally with time, while θ_2^* was kept constant. Above the tropopause, the phase was set equal to the sun; that is, the scale factor, SS , multiplying θ_1^* , θ_3^* was unity at the solstices and zero at the equinoxes. At lower levels (600 and 300 mb), a phase lag of 3 weeks was included since the primary heat source of the tropo-

sphere is the surface of the earth. The observed phase lag varies considerably between the centers of continents, coastal regions, and the oceans. The value chosen, combined with the time constant of heating, should provide a time lag in the temperature field of about 1 mo behind the sun. This scale factor, ST , was also used for all components of the nonzonal heating. Thus,

$$SS = \sin \frac{2\pi}{365} (t_0 - t)$$

$$ST = \sin \frac{2\pi}{365} (t_0 - t + 21)$$

where t_0 is chosen so that $SS=1$ on $t=\text{December } 22$ (t in days).

3. MODEL ENERGETICS

Much of our later analysis will be based upon the changes in the different forms of energy, in the manner of many observational studies. We note, however, that many of these studies are of the energetics of only part of the globe, often not even an entire hemisphere; thus, differences in definitions will exist.

We will evaluate the global energetics, thereby averaging the summer and winter regimes, but will also consider each hemisphere separately. Whereas the global kinetic energy, K , is the mean of the hemispheric values (per unit area), a similar relation may not hold for available potential energy A . The latter depends on the deviation of the temperature field from the mean for the layer and thus depends on the area over which the mean is determined. We shall use a global mean, as does Newell et al (1970), so that the global A is the mean of the hemispheric values. This is not the case in most observational studies.

Certain problems arise in expressing the energy equations in spherical harmonics on a hemispheric basis. The truncation of the spectral series prevents nonlinearities from overly dispersing the spectra but may cause mathematical equalities to no longer hold when expressed in truncated form. The global expressions for the zonal and eddy forms of A and K and the conversions between them have been given by Peng (1965) and Trenberth (1972).

In the N.H. expressions, boundary terms are introduced in both A and K equations. However, because of the truncation of the series, exchanges of energy may also take place between the hemispheres without involving a flux of energy across the equatorial boundary. The abbreviated form of the conversions for the N.H. are

$$\frac{\partial AZ}{\partial t} = GZ - CZA - CAZ + BAZ, \quad (18)$$

$$\frac{\partial AE}{\partial t} = GE - CEA + CAE + BAE + AF, \quad (19)$$

$$\frac{\partial KZ}{\partial t} = CZK + CKZ - DZ + BKZ, \quad (20)$$

and

$$\frac{\partial KE}{\partial t} = CEK - CKE - DE + BKEH + BKE + KF. \quad (21)$$

The notation used is a modification of the conventional representation. GZ, GE and DZ, DE refer to generation and dissipation, as usual. However, instead of CA (conversion of AZ to AE) for the global case, we have CAZ [conversion of (AZ)_{N.H.} into (AE)_{GLOBAL}] and CAE [=the conversion of (AZ)_{GLOBAL} into (AE)_{N.H.}] for the N.H. conversions. Similar relationships apply for CE, CK, and CZ. BAZ, BAE and BKEH refer to horizontal fluxes of these quantities across the Equator. BKE and BKZ refer to the exchange of kinetic energy due to orographical distortion. AF and KF denote the exchange between the hemispheres through nonlinear interactions between the waves.

A more detailed analysis by levels requires the introduction of the vertical fluxes of geopotential energy, denoted here by $V\Phi Z$ and $V\Phi E$. Each of the above terms is considerably more complex than the corresponding global expression, and a complete detailed analysis has been given by Trenberth (1972).

Figure 3 shows the four-box diagram usually used for presenting energetics analyses. Each box is isolated since the hemispheres are not closed energetically because of the boundary at the Equator and the limited degrees of freedom caused by truncation of the spectral series. The change necessary for the contributions into each box to balance is given in parentheses below the value of the form of energy.

The model atmosphere will be subdivided into three regions for comparing the model energetics with the atmosphere. The layer 1000–200 mb will be considered as the troposphere, 200–20 mb as the lower stratosphere, and the region above 20 mb as the upper stratosphere. The last region also includes the mesosphere. The divisions are necessarily somewhat artificial, but they will suffice for our purposes.

4. PRELIMINARY SOLUTIONS

a. Symmetric Integration

Following the conventional procedure for setting up a numerical experiment with an atmospheric general circulation model, we allowed a symmetric zonal flow to develop at equinoctial heating. After 60 days, the annual heating cycle was introduced into the model and a computer run was made for 1 yr without eddies.

These results are presented since they provide a background for considering the effects of the eddies in the full-scale response of the model. As both hemispheres are identical, only 6 mo are considered. Temperature and wind fields are presented at 30-day intervals, corresponding to the dates shown in figure 4. A schematic diagram of the meridional circulation accompanying these fields is also given. These contours were drawn to represent stream-

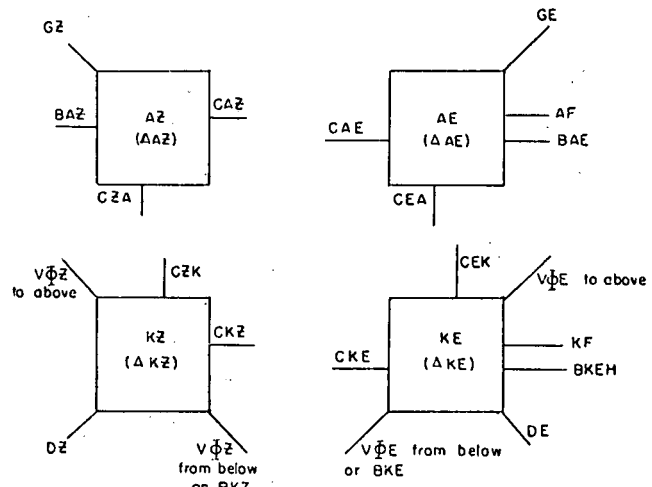


FIGURE 3.—Representation of energetics in the model.

lines, but they are not spaced to account for the strength of the flow.

The maximum winds appeared a few weeks after the solstice with westerlies of 180 m/s and easterlies of 40 m/s. The easterlies are not as strong as observed, nor do they extend to sufficiently low levels. This was expected to be improved by the inclusion of eddies, which should also reduce the westerly maximum.

The greatest amplitude (0.25 m/s) of the meridional velocity at the upper levels in our model occurred near 60 km in April and October. The differential heating near the stratopause, which is the forcing field for the motions, is weak prior to the solstice and reverses shortly thereafter due to the progress of seasons. Hence, the meridional circulations are weaker at the time of the solstice. The strongest meridional flow in the troposphere occurred during January and July.

It is of interest to compare figure 4 with the stratospheric Hadley circulations presented by Leovy (1964). He considered the zonally symmetric circulation at the solstice as driven by heating in that region, subject to eddy fluxes of heat and momentum, with a lower boundary at 22.5 km. Thus, tropospheric influence on the upper atmospheric circulation was neglected. The introduction of the eddy fluxes may make his solution more comparable to the period prior to the solstice; but, even if the maximum meridional circulation in our model is considered, the strength is still much less than half that found by Leovy. Some differences are caused by the upper boundary in this model, but they are primarily due to the inclusion of the troposphere, which allows the presence of a substantial return flow at the low levels.

b. Baroclinic Growth Rates

To obtain a model that behaved like the real atmosphere, we chose parameters from real data. However, because of the truncation of the spectral representation and the limited vertical resolution, it was recognized that the model would not correspond exactly and might even have a solution differing considerably in some respects.

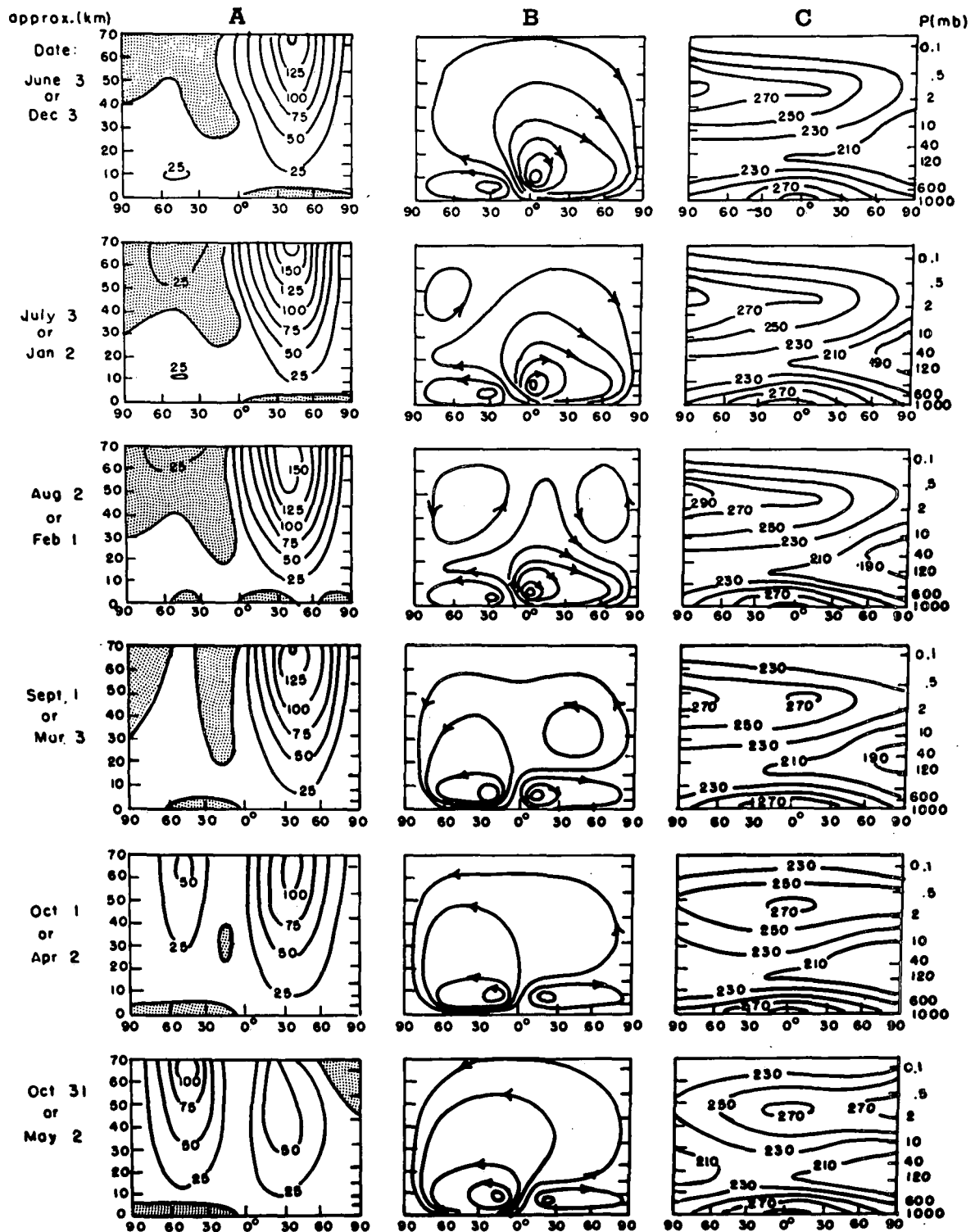


FIGURE 4.—The (A) zonal wind (m/s)—Easterlies are shaded, (B) schematic meridional wind streamlines, and (C) zonal temperature ($^{\circ}\text{K}$).

Therefore, we chose somewhat different parameters to gain the best resemblance between those features of the flow deemed important and used a similar but further simplified model to perform a baroclinic instability analysis. This was a three-layer model, formulated on a sphere with a realistic basic state that contained both vertical and horizontal shear. To eliminate barotropic effects, we considered only single modes of each wave. Details of the analysis are given by Trenberth (1972).

Results indicate that, in the long-wave region of instability first noted by Green (1960), the growth rates may be much greater than indicated by a beta-plane analysis.

A lower static stability in the lower troposphere destabilizes all waves. An increase in the static stability in the upper troposphere, however, tends to destabilize the short waves (wave number greater than 5) and stabilize the long waves. Green (1960) found a similar result when

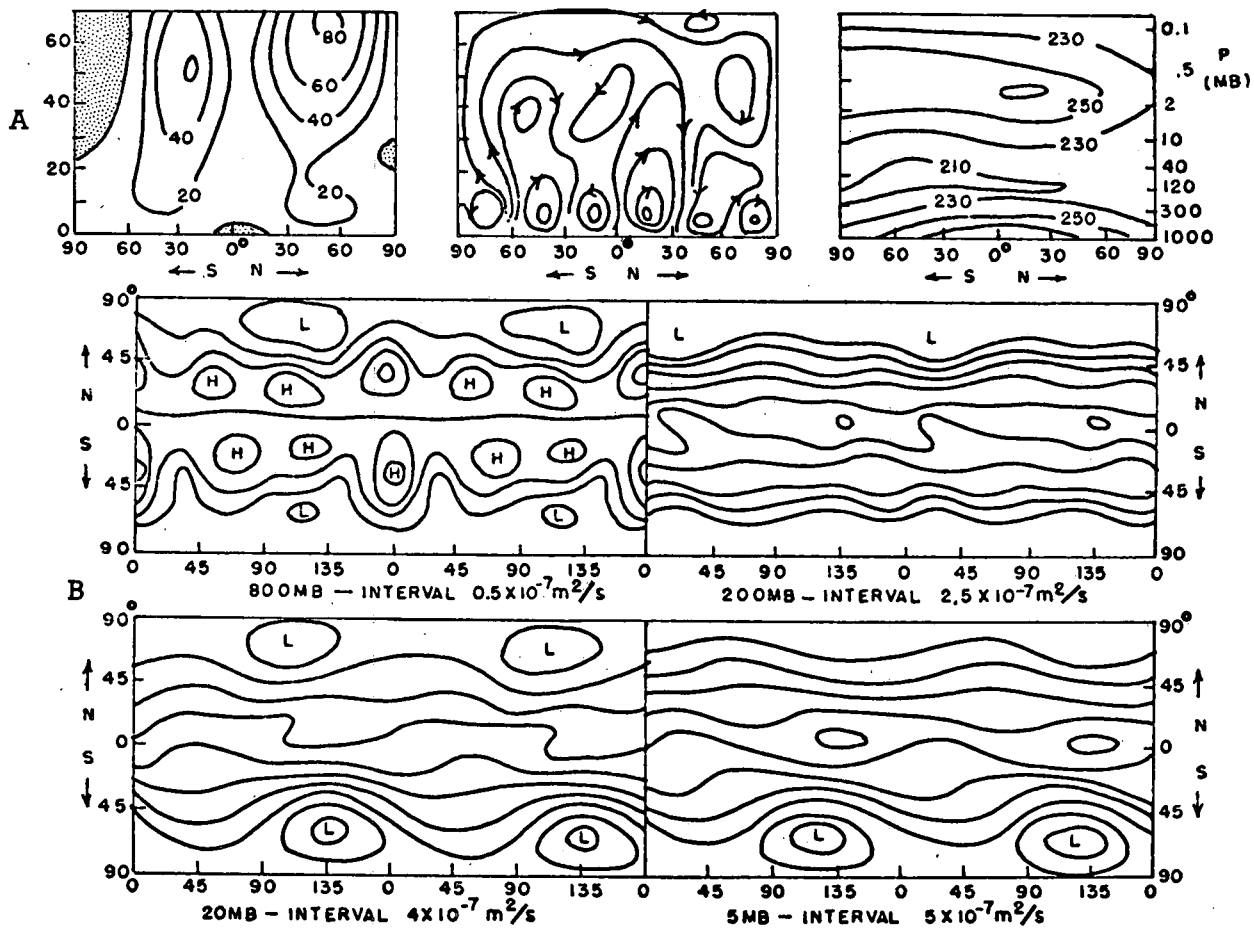


FIGURE 5.—(A) same as figure 4 for day 25 (Oct. 26) and (B) streamlines at selected levels as a function of latitude and longitude on day 25.

comparing the effect of a rigid top to a stratospheric layer. Accordingly, to offset the effects of the short-wave cutoff that results from the finite vertical resolution, we decreased the static stability values slightly at 600 mb and increased them slightly at 300 mb to increase the growth rate of wave 6 to a more realistic value. Wave 6 is a wave commonly regarded as "baroclinic," whereas wave 2 is likely to have the different characteristics of very long waves. Wave 4 should be close to the transition point.

c. Introduction of Eddies

Perturbations in waves 4 and 6 were introduced at all tropospheric levels into the zonally symmetric solution corresponding to October 1. There was neither orography nor nonzonal heating included that would distinguish the hemispheres, but, for convenience, we shall refer to the spring hemisphere as south and autumn hemisphere as north.

Both waves grew by baroclinic processes while interacting to produce a perturbation in wave 2. The subsequent growth of these waves may be seen in figure 7. Wave 2 was strongly baroclinic in the sense that $AZ \rightarrow AE \rightarrow KE$ continued at a much greater rate than KE was dissipated in the troposphere. As a result, the increase in K_2 (i.e., the kinetic energy in wave 2) occurred in the stratosphere as large quantities of energy were propa-

gated upward. By day 20, this had reached the uppermost level (0.05 mb) and was trapped by the upper boundary. The vertically propagating energy was accompanied by a polewards transport of heat ($AZ \rightarrow AE \rightarrow KE$), which induced meridional cells ($KZ \rightarrow AZ$), and a downward flux of geopotential by the zonal flow. As a result, the zonal westerlies weakened considerably.

In the spring hemisphere, the trapping of energy at the uppermost levels resulted in the formation of easterlies at high latitudes along with a reversal of the mean temperature gradient. Then this part of the atmosphere responded in the manner of the lower stratospheric region of the atmosphere and was driven by absorption of the vertically propagating energy $V\Phi E_{UP} \rightarrow KE \rightarrow AE \rightarrow AZ \rightarrow KZ \rightarrow V\Phi Z_{DOWN}$, which continued to modify the zonal flow. Thus, in the spring hemisphere, events of a sudden warming nature took place.

In the N.H., similar events were taking place to a lesser degree. A warming did occur some 5 days after that in the S.H., but in this case it was centered at the 10-mb level and was not affected by the upper boundary.

The situation on day 25 (Oct. 26) is presented in figures 5A and 5B. The former may be compared to the corresponding figure when no eddies were present (fig. 4). The most obvious change is the breakdown of the single Hadley cell in the troposphere of each hemisphere into three-cell systems, and the appearance of a two-cell

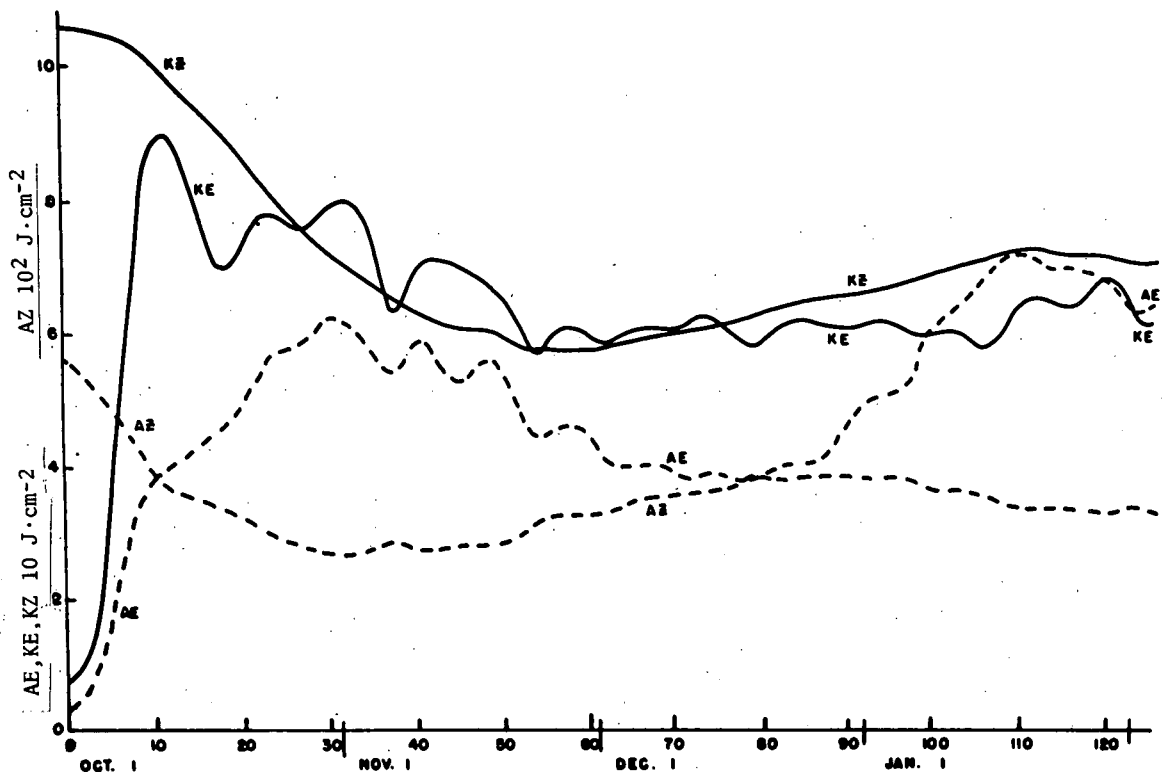


FIGURE 6.—Daily variation of the vertical integral of global forms of energy in experiment A.

system in each hemisphere in the stratosphere combined with the global pole to pole Hadley circulation. The westerlies have been weakened in the N.H. and the easterlies are more extensive in the S.H.

Figure 5B shows the streamlines at representative levels. Since only even wave numbers were included, the pattern repeats itself after 180° of longitude. The 800- and 200-mb levels reveal tropospheric flow patterns. The 20-mb chart is similar to the 70-mb chart except for a phase shift in the waves, and the levels of 5 mb and above are similar. The closed low-pressure systems extend from 70 mb to the top of the model in the S.H. with a westward slope with height, but a closed Low is present only at the 70- and 20-mb levels in the N.H.

The above discussion considered events triggered by the introduction of eddies into the troposphere of a model with a lower stratosphere unlike that observed. However, apart from the unrealistic way in which the events began, the stratospheric adjustment was not unlike that observed during sudden warmings. Therefore, it reinforces our assertion that an abrupt large-scale change in the forcing of the stratosphere from below would produce such changes (Trenberth 1973).

5. RESULTS OF EXPERIMENT A: NO NONZONAL FORCING

Whenever such a simple model as ours is used to investigate a complicated dynamical system, the capability of duplicating a given phenomenon does not necessarily imply the correctness of the model in describing the mechanism responsible for the real phenomenon. In this

section, points of agreement and deficiencies in the model are discussed, the likely causes of the deficiencies are deduced, and the suitability of the model for our experiments is ascertained. Some new results are presented, but those relating to the sudden warming event will be given elsewhere (Trenberth 1973).

In experiment A, all nonzonal forcing was excluded so that the winter hemisphere should more closely resemble a S.H. winter. In the following discussion, however, we shall continue to refer to the winter hemisphere as north.

Figure 6 presents time series of the vertically integrated global forms of the zonal and eddy energy. Figure 7 shows the breakdown of the eddy terms into wave numbers. These diagrams indicate that the model does not become adjusted to the eddies and approach a statistically steady state with a seasonal trend superposed until at least day 50.

a. Zonally Averaged Fields

Figure 8 shows the zonal temperature and wind fields and meridional cell streamlines at monthly intervals for the dates shown. These dates are the same as those for the similar presentation without eddies in figure 4. The zonal wind and temperature fields do not change very rapidly, and daily values are representative of the monthly means. The meridional circulation is subject to shorter period changes, and thus 5-day mean values are presented. The principal features are evident from these diagrams.

The latitude and strength of the model tropospheric jet in both hemispheres is in agreement with observations given by Newell et al. (1970). Easterlies are present in the model troposphere Tropics at 800 mb but are absent

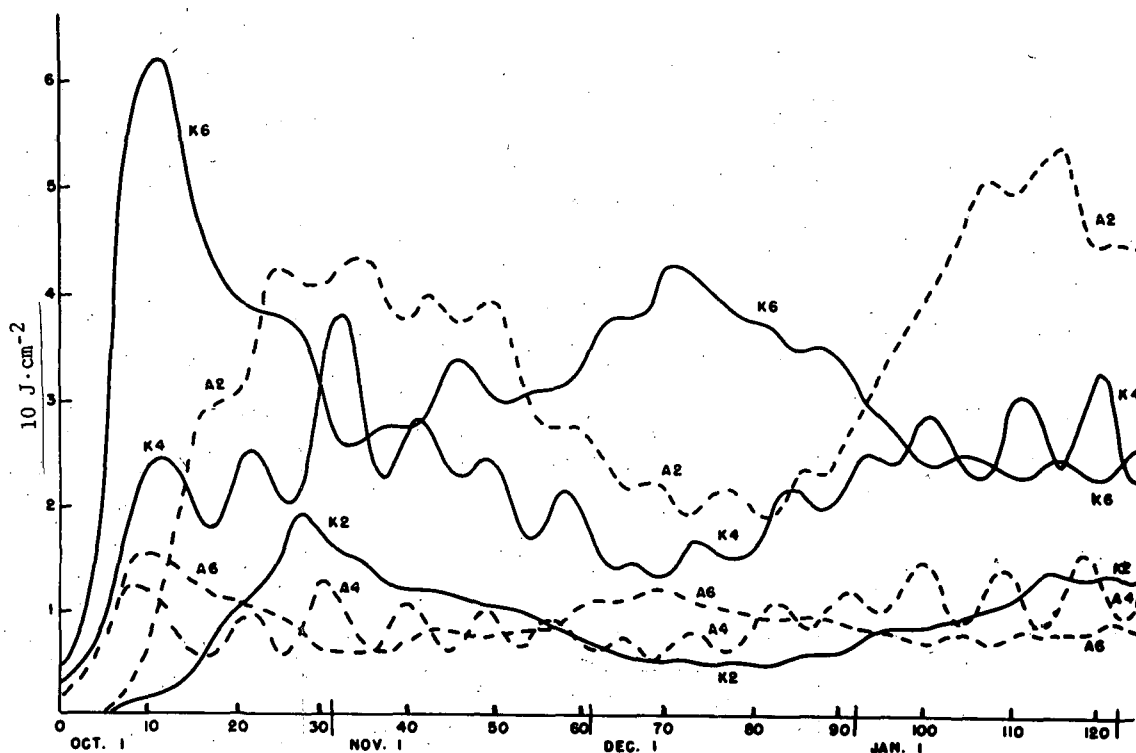


FIGURE 7.—Same as figure 6, for eddy components in waves 2, 4, and 6.

above that level. This extension of the winter westerlies into equatorial regions at most levels above 800 mb is a feature of the model that is not observed in the real atmosphere. A single maximum of easterly winds is present at the lowest level where the Hadley cells in each hemisphere converge. In reality, the doldrum region exists there with the trade winds forming a double maximum on either side.

The pattern of the model upper atmospheric winds is in general agreement with the observed (Murgatroyd 1970). The secondary easterly maximum at 70 km in low latitudes is not observed, but agreement exists with the location and strength of the primary easterly maximum. At lower levels, however, the maximum observed easterlies extend into low- to midlatitudes, whereas the model maintained strong easterlies at high latitudes.

The location of the westerly jet maximum was at either 0.2 or 0.05 mb (60 or 70 km) as is found in the atmosphere. The maximum winds of 140 m/s, although more realistic than the 180 m/s in the no-eddy run, are still too strong. In fact, the strength of the westerlies throughout the N.H. stratosphere is slightly greater than the observed mean winds. The westerly wind maximum extends down into the lower stratosphere at lower latitudes than observed and has a tendency to be connected to the tropospheric jet.

Overall, therefore, the wind field and its seasonal variation has been well simulated. We also find agreement in most respects between the model temperature field and the observed (Murgatroyd 1970, Newell et al. 1970).

At 600 mb, the model temperature gradient between the Equator and pole was 50°K in winter and 30°K in summer. As values representative of the lower troposphere, they

compare favorably with the observed. When compared to the symmetric circulation run in figure 4, we find the temperature gradients to have been reduced by about 5°K. The means by which this was accomplished was for the most part poleward heat transports by the large-scale eddies.

The most notable discrepancies in the model temperature field are in the lower stratosphere. The tropical tropopause is not as cold and intense as observed. The increasing temperatures toward the pole are correctly simulated in the summer lower stratosphere, but the same pattern is also seen in the winter hemisphere. In the atmosphere, a midlatitude temperature maximum is found in winter.

The three-cell tropospheric circulation was present throughout the experiment and showed the dominance of a direct cell extending across the Equator from the winter hemisphere. The rising motion reached a maximum near 10°S with subsidence in the subtropics. These features resemble the observed pattern (Newell et al. 1970) remarkably well. The p velocity of the rising motion in the convergence region averaged about 19×10^{-5} mb/s at 600 mb, which is more than twice the value found for the symmetric run (fig. 4).

The Ferrel cell in the midlatitudes of both hemispheres seems weaker, and the high-latitude direct cell stronger than observed (the intensities were not computed). These features are particularly noticeable in the lower stratosphere where a two-cell circulation in each hemisphere should be formed from the extension of the low-latitude Hadley cell and the midlatitude Ferrel cell to higher levels (e.g., Manabe and Hunt 1968, Holloway and Manabe 1971). This did occur at times in the model when the eddies

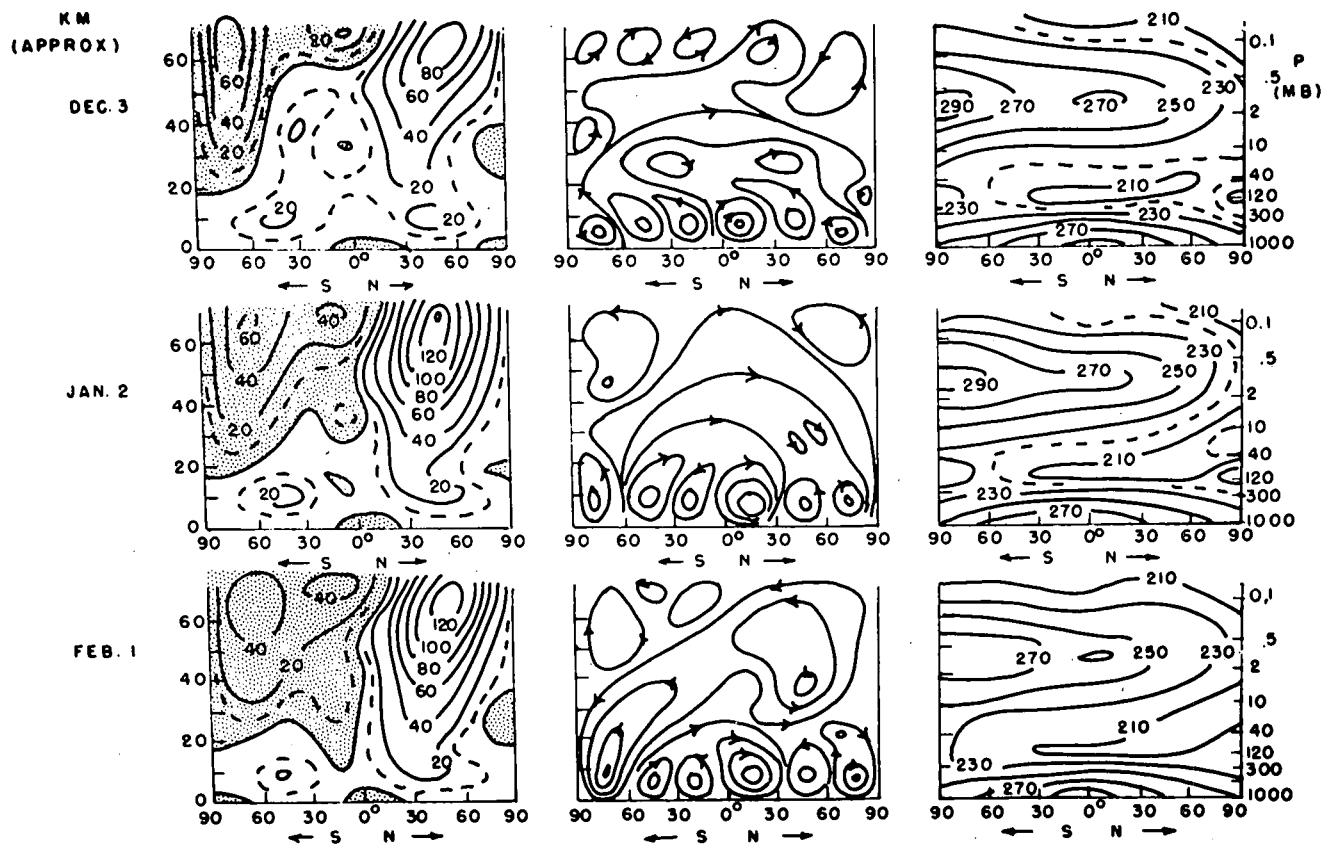


FIGURE 8.—Same as figure 4 for experiment A.

TABLE 3.—Zonal average of the northward meridional velocity (cm/s) for the summer hemisphere

Level	Latitude (°S)	60	30	0
0.05 mb		-7	-0	15
0.2 mb		1	1	5
1 mb		-2	4	9
5 mb		6	5	11
20 mb		0	9	12

were particularly strong (fig. 5).

In the upper atmosphere, the meridional circulation tends to be a global Hadley cell, although variations did exist. The beginning of the reversal of this cell can be seen in figure 8 on January 2. Although the heating field begins to reverse at this time, the change was primarily due to the eddies, as may be seen by comparing the meridional circulation for February 1 with the corresponding time in figure 4.

Newell (1968) has speculated on the meridional motions in the upper atmosphere. By neglecting the effects of eddies in a steady-state solution, he deduced rising motions to be present in the summer hemisphere at 50 km, accompanied by equatorward drifts of 3–5 cm/s. In the model, the presence of eddies produced daily changes in the Hadley cell, so that the 5-day mean values were weaker than the daily values. In table 3, the meridional velocity is given at each level in the upper stratosphere for summer

for the 5-day period centered on January 2. Positive values are northward.

The zonally averaged vertical motion accompanying these values at 2 mb (43 km) was greatest in midlatitudes, measuring about -10^{-7} mb/s (roughly 0.4 mm/s). At 0.5 mb (53 km), the maximum of about -1.5×10^{-8} mb/s (about 0.3 mm/s) was in low latitudes.

These values are of the same order as those deduced by Newell. They are also similar to those in our solution without eddies for this date but are much lower than the values found by Leovy (1964); see the discussion in subsection 4a.

b. Energy Budget

Figures 9A and 9B show the four-box diagrams for the troposphere (1000–200 mb), lower stratosphere (200–20 mb), and upper stratosphere (above 20 mb). The meaning of the diagram is explained in figure 3 and section 3. The global, as well as N.H. (winter), and S.H. (summer) energetics are shown for the months of December (fig. 9A) and January (fig. 9B). Energy values are 10^{-2} J·cm⁻² and conversions 10^{-7} J·cm⁻²·s⁻¹.

All calculations were checked by comparing the net contribution of the conversion terms to each box with the measured change in each energy component. In the later experiments, B, C, and D, the energetics calculations were made once each day and the agreement in the above check procedure was excellent. In this experiment, the hemispheric energetics were computed with a 2-day

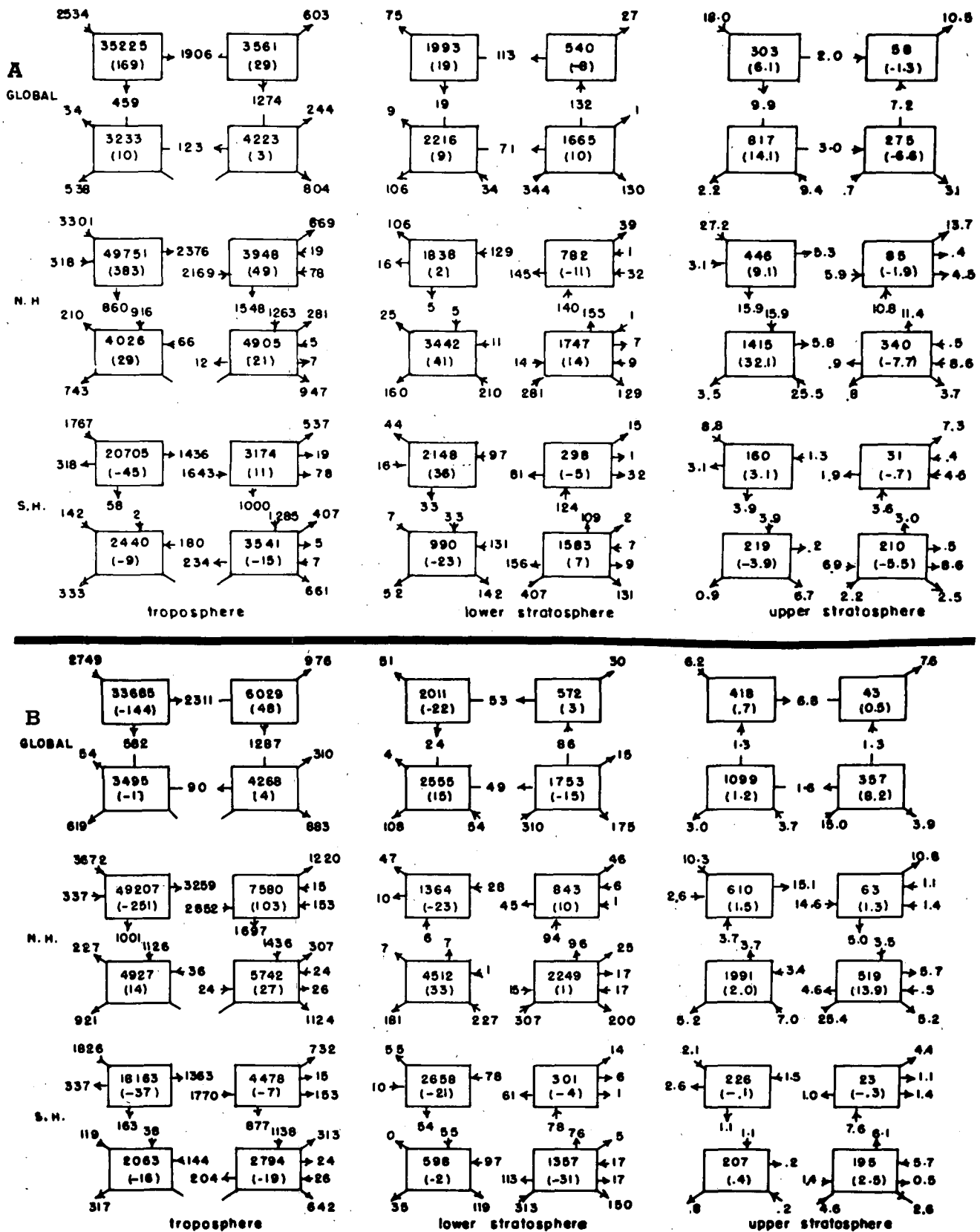


FIGURE 9.—Energetics in experiment A for (A) December and (B) January. Energy values are $10^{-2} \text{J} \cdot \text{cm}^{-2}$ and conversions are $10^{-7} \text{J} \cdot \text{cm}^{-2} \cdot \text{s}^{-1}$.

interval, and some small sampling errors were apparent. The tropospheric values of AZ, KZ, and KE, in both hemispheres show good agreement with the observed (Newell et al. 1970), when allowance is made for differ-

ences in the regions. The ratio of KE to KZ is close to unity, as may also be seen in figure 6. This observed feature of the atmosphere has been lacking in the more sophisticated primitive-equation models (e.g., Manabe et al. 1970).

Oort (1964*b*) finds AE to be about twice the value of KE and KZ. Our model values, similar to those found in the Geophysical Fluid Dynamics Laboratory (GFDL) models that exclude nonzonal effects (Manabe et al. 1970), are probably too low. This is most likely due to the lack of waves 1 and 3 in the model, which along with wave 2 contain most of the AE in the atmosphere. Figure 7 indicates how the ratio of AE to KE changes with wave number. It also shows a marked increase in A2 going into January, which is reflected in the monthly values in figure 9. The lack of nonzonal forcing in this experiment is most likely a factor, but this will be remedied later.

The uncertainty in the conversion terms for the atmosphere is apparent from the wide range of values present in the literature. Further confusing the issue is the natural variability of the atmosphere itself. Our model troposphere compares favorably in all but three conversions. The conversion CZ (AZ→KZ) is too large in the model in winter, indicating the dominance of the direct cells in the meridional circulation. This is partly due to truncation as noted in subsection 5e. As a result, the conversion CK is less than observed in the winter hemisphere.

GE has the opposite sign in the model from that observed because of the lack of nonzonal heating in this experiment. This feature is also present in the GFDL dry models where the hydrologic cycle is omitted (e.g., Manabe et al. 1970). The presence of nonzonal heating should decrease GE; but, without water vapor in the model, we cannot obtain the gain in AE in transient waves due to condensation east of the trough, as described by Manabe et al. (1970).

The intensity of the energetics is indicated by the total production of A, total dissipation of K, or the conversion between them (CZ+CE). In a long-term average, these should all be equal. In January, there was a marked increase in the intensity of the N.H. tropospheric circulation. As may be seen from figure 7, this was largely brought about by wave 2. The resultant large increase in AE was accompanied by a decrease in AZ, giving rise to a maximum AZ in December. This kind of response has also been noted in the atmosphere by Krueger et al. (1965), who found a double maximum of AZ in December and March to be normal. The increased intensity resulted in an increased eddy flux of energy into the lower stratosphere and particularly into the upper stratosphere.

The model lower stratosphere energetics of both summer and winter hemispheres are similar in overall characteristics and resemble those of Manabe and Hunt (1968). The circulation is driven from below by the vertical eddy flux of geopotential. Energetics studies of this region (e.g., Dopplick 1971) reveal the baroclinic nature of the winter lower stratosphere, which is not apparent in the model. This point was mentioned in the previous section as a deficiency of the model simulation of the temperature field.

In December, the Hadley cell driven by the heating field was dominant in the upper stratosphere; therefore, the symmetric part of the flow prevailed. KZ increased throughout the month to reach a seasonal peak. In January, GZ was negative above 5 mb and the reversal

TABLE 4.—Gain in energy by N.H. through interhemispheric exchange ($10^{-7}J \cdot cm^{-2} \cdot s^{-1}$)

	Troposphere	Lower stratosphere	Upper stratosphere
Dec.	-79	+13	+0.6
Jan.	+20	-7	-3.3

in the meridional circulation produced a source of AZ through the conversion CZ. The changes were stimulated by the increased eddy flux of energy into the region from below. As a result, CA, CE, and CK all became positive. However, the changes in AE and KE were not particularly great, although the change in the energy cycle was pronounced. The change in the energetics of the region was associated with the sharp increase in wave 2 energy in the troposphere that we noted earlier, and it was largely a coincidence that it occurred at about the time of the solstice.

The energetics of the upper stratosphere in the model of Manabe and Hunt (1968) is qualitatively similar to that of our January simulation of the winter hemisphere.

In the summer upper stratosphere, energetics conversions are small in comparison and seem reasonable. Since the model easterlies were less extensive than observed, however, the energetics are not completely representative of an easterly regime. Thus the horizontal boundary fluxes into the region are taking place mostly in westerlies at the Equator, and the vertical fluxes are occurring in the low to midlatitude westerlies at 20 mb.

Newell (1965) speculated that a source of energy for the summer upper stratosphere may be required since GZ is small and the vertical flux of energy would be absorbed in the lower stratosphere. He concluded that this energy might be derived from the winter hemisphere.

As is apparent from figure 9, the month of December was dominated by the symmetric terms driven by the differential heating in the region. In January, this forcing was no longer effective, and GZ became negative at the higher levels. All conversions were small, but the increase in the importance of the eddies is evident. The source of the eddy energy was from a vertical flux, while the horizontal boundary fluxes do not seem to be of importance in the model. The issue is clouded, however, since eddy motions may have been induced in the S.H. by the more vigorous motions in the N.H. winter circulation through unrealistic restraints imposed on the motions by truncation of the spectral modes.

If we now briefly consider the boundary fluxes at the Equator and differences in conversions such as CAE and CAZ, we may find the interhemispheric exchange of energy. Table 4 shows this change in AZ+AE+KZ+KE in $10^{-7}J \cdot cm^{-2} \cdot s^{-1}$ for the winter hemisphere in December and January.

These values are small compared to the other conversions, and the changing sign of the exchange in each month indicates that the transport is not significant. Certain terms are large and consistently in one direction but are balanced by other terms. For example, contribu-

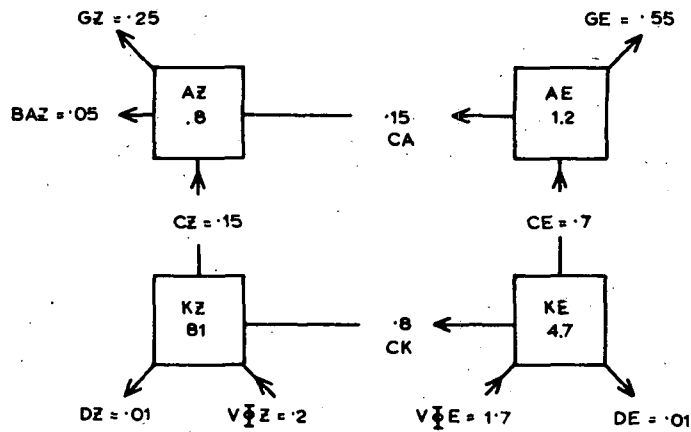


FIGURE 10.—Same as figure 9 for N.H. December and January mean values in layer above 0.2 mb (61 km).

tions to AZ in the troposphere for both months were such that BAZ is large and positive into the N.H. and is supported by the difference between CZA and CZK, but the contribution is cancelled to a large degree by the difference between CAZ and CAE.

Most energetics studies of the troposphere have ignored boundary fluxes of energy. Dopplick (1971) found them to be small in the lower stratosphere. Our model showed most of these terms to be small or to be cancelled by another term of similar nature.

c. The Mesosphere in Winter

Included within the upper stratosphere, as we have defined it, is the region above 60 km, which is actually part of the mesosphere. Newell (1968) discussed the energetics of this region distinct from the layer below.

Using a diagnostic approach, he deduced the region to be one of forced motions somewhat analogous to the lower stratosphere. The forcing could either originate from the baroclinic waves generated in situ in the 25–60 km region, or from leakage of the vertically propagating energy from the troposphere.

In our model, the top layer did indeed behave in this manner, although it was most likely affected to some degree by the upper boundary. Unlike all layers below, GZ was negative for both months. The details of the energetics of this layer (from 0.2 mb (61 km) to the top of the model) are shown in figure 10. The values of AZ, AE, and KE changed little throughout the period, but KZ increased to a peak in mid-January and showed a net gain for the period of nearly $10^{-7} \text{J} \cdot \text{cm}^{-2} \cdot \text{s}^{-1}$.

The horizontal boundary terms at the Equator were small and are not shown except for BAZ. The conversion terms are average values [e.g., $\text{CK} = \frac{1}{2}(\text{CKE} + \text{CKZ})$] and are accurate to $\pm 0.1 \times 10^{-7} \text{J} \cdot \text{cm}^{-2} \cdot \text{s}^{-1}$.

As may be seen from this figure, the energetics are similar to that of the lower stratospheric region and are driven from below by the vertical flux of eddy geopotential energy. Throughout the period, the highest temperatures in the N.H. at 0.1 mb ($\approx 66 \text{ km}$) were in midlatitudes near 45°N . Thus the structure of this region, with cold temperatures at the Equator and polar regions and a midlatitude

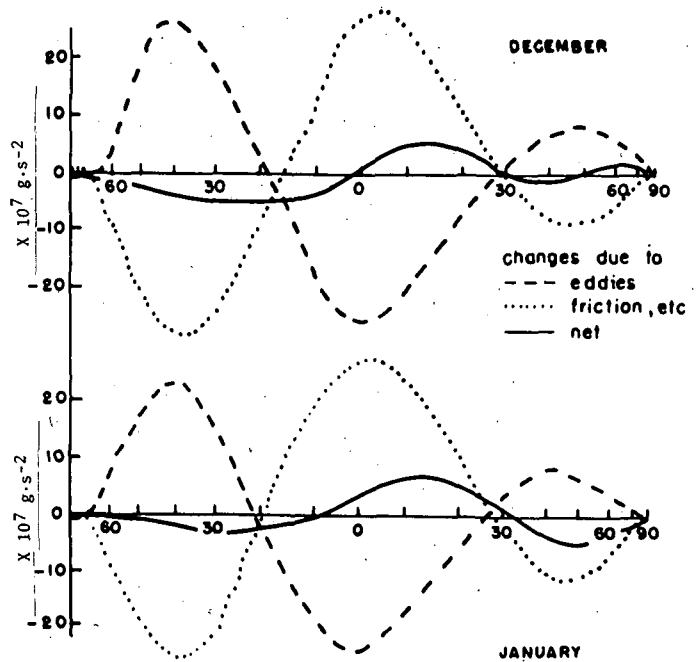


FIGURE 11.—Angular momentum budget.

maximum, is like that observed for the winter lower stratosphere (but not present in the model lower stratosphere). See figure 8.

d. Angular Momentum Budget

The angular momentum budget has been evaluated and the net change for a vertical column, averaged around a latitude circle, is shown as a function of the sine of the latitude in figure 11. This represents the net balance due to contributions from the friction mechanism and the redistribution of angular momentum by the eddies.

While the angular momentum is conserved on a global basis (i.e., the positive and negative areas under the friction curve balance), there is nowhere near a balance on a hemispheric basis. Thus, there is a large eddy transport of angular momentum across the Equator out of the winter hemisphere. This feature has also been found in the real atmosphere (Kidson and Newell 1969). The flux into the summer hemisphere in the model is entirely due to the eddies and is about $10 \times 10^{25} \text{g} \cdot \text{cm}^2 \cdot \text{s}^{-2}$ in December, and $6 \times 10^{25} \text{g} \cdot \text{cm}^2 \cdot \text{s}^{-2}$ in January, which, surprisingly, agrees with the values of Kidson and Newell.

The seasonal variation in the wind fields is revealed by the net gain in westerly momentum in the winter hemisphere while being offset by the increase in easterly (or decrease in westerly) momentum in the summer hemisphere. In the N.H., the net change curve illustrates the shift in latitude and increase in the westerly maxima as both the tropospheric and stratospheric jets intensify and move equatorward. These features are also evident from figure 8.

The above aspects of the wind fields and angular momentum budget clearly cannot be reproduced in models that do not incorporate a seasonal cycle or that are symmetric about the Equator while using the truncated spectral representation.

The details of the curves in figure 11 do not resemble those for the atmosphere in the Tropics. [See, for example, the frictional torque on the atmosphere given by Newton 1971 and the contributions of the eddies, mean cell, and frictional torque in the GFDL model (Manabe et al. 1970).] The lack of a doldrum region in the easterlies was noted earlier, and this is reflected in the frictional torque profile. The net angular momentum transported by the mean meridional cells in low latitudes is significant in the atmosphere but is omitted by the quasi-geostrophic formulation. The pattern poleward of 35° is, however, in qualitative agreement with observation.

The largest eddy transports are at 200 mb, revealing the importance of large-scale eddies in maintaining the structure of the tropospheric jet. No such transports appear to be of significance in the stratosphere of the model, however. Manabe and Hunt (1968) noted the tendency for the changes in this region due to eddies and those due to the meridional circulation to balance, but the indirect cell that dominated the high-latitude stratospheric region of their model was mostly absent here.

e. Source of Discrepancies

Many of the differences between the model and the real atmosphere were expected. Some are probably due to the lack of nonzonal forcing and may be remedied in later experiments. Defects caused by the lack of water vapor and clouds in the model are not very large in the mean zonal fields but were noticeable in the energetics. The quasi-geostrophic formulation is deficient in the Tropics. The lack of any net transports of angular momentum by the meridional cells is a feature of a quasi-geostrophic model that was particularly evident in the angular momentum budget.

Manabe and Hunt (1968) found the general features of the lower stratosphere to be better simulated with a high-resolution model. The vertical resolution of our model will probably also preclude the possibility of linear baroclinic instability in the stratosphere (Murray 1960, McIntyre 1972).

The external heating used here is undoubtedly a major source of discrepancy. This formulation, however, seems sufficient for the purposes of the experiment, although the parameterization could very likely be improved. The strength of the westerlies in the upper stratosphere and the location of the maximum easterlies and westerlies in each hemisphere of the lower stratosphere can probably be improved in this way.

The truncation of the spectral representation of the variables is undoubtedly another major source of error. Since we kept six modes to represent the zonal flow but only three to represent each wave, the added degrees of freedom act to enhance the symmetric effects and increase the efficiency of the mean cells relative to the eddies.

Apart from this balance, some atmospheric events may have been excluded by the truncation of the modes. For example, Kikuchi (1969) found a four-cell meridional structure to be present in the troposphere when blocking occurs.

Some of the above defects in the model were expected and regarded as acceptable. The general performance of the model, in view of the many simplifications, is very good. The simple manner in which the seasonal variation was introduced proved very successful. However, some defects may affect the results of the experiments planned. The effects of the eddies on the stratosphere were small, and, since we are interested in the vertical propagation of energy by the eddies, we may expect to obtain an underestimate. In addition, the winter lower stratosphere of our model does not have a baroclinic region at high latitudes; our structure is less favorable for vertical energy propagation.

6. EFFECTS OF ANNUAL HEATING CYCLE

A mechanism, considered to be a distinct possibility in providing an abrupt change in the activity of the planetary scale waves and thus in forcing the stratosphere from below, arises from the existence of an index cycle in the very long waves.

Annual cycle dishpan experiments (Fultz et al. 1959, Lorenz 1963) have demonstrated that the wave number of the flow is determined by a thermal Rossby number, which depends on the meridional temperature gradient. As the temperature gradient increases, the wave number of the flow decreases. This is explained by the following mechanism. As the meridional temperature gradient increases, the baroclinicity and hence the intensity of the circulation increases. A greater vertical transport of heat and energy by baroclinic eddies results, which is not offset by radiational cooling, thereby causing an increase in static stability. This in turn causes the wavelength and shear required for baroclinic instability to increase. Bryan (1959) found that this process may exist in the atmosphere and affect the wavenumber that dominates the flow. The waves also undergo a vacillation process that has been likened to the atmospheric index cycle. Both act to reduce the meridional temperature gradient.

The index cycle refers strictly to variations in the strength or latitude of the zonal westerlies. In terms of energetics, however, this index may be interpreted as a cycle in the intensity of the energy conversions and energy amplitudes. In the extreme case of blocking, some conversions may even reverse direction. In this way, the long waves are subject to an index cycle, although it is not clear whether or not the length of such a cycle is less than one season.

The meridional temperature gradient increases as winter progresses until some time after the solstice. Miyakoda (1963) found the peak gradient in the troposphere and lower stratosphere to occur just prior to a sudden warming.

In our model, we noted that a marked increase in the intensity of the tropospheric circulation produced a large increase in AE and a decrease in AZ toward the end of December. However, the heating field was acting to produce the lowest polar temperatures and a maximum in AZ sometime after mid-January, as occurred in the integration with eddies excluded.

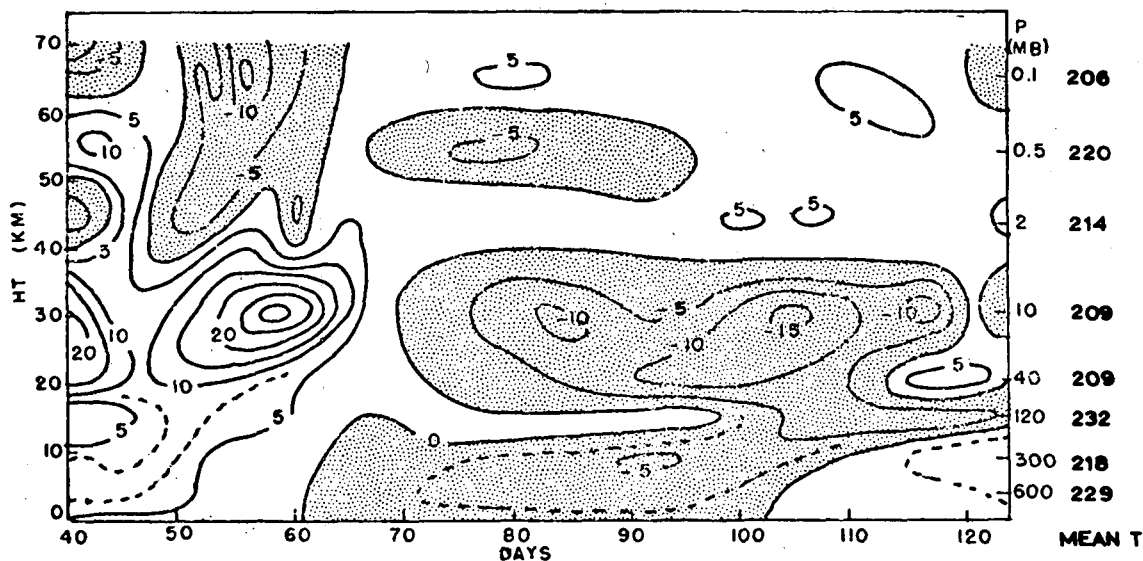


FIGURE 12.—Deviations from level mean temperatures at 90°N. Mean value at right.

Figure 12 shows the time variation of the polar temperature at 90°N. The mean from days 40 to 125 has been extracted and is shown at right. Here we see that the lowest temperatures occur at the end of December in the troposphere, and some 10 days later at 10 mb.

Figure 7 shows the increased eddy activity to be in wave 2, resulting in a marked increased role in wave 2 and wave 4, while the kinetic energy in wave 6 declined in January. Associated with this was a marked increase in the vertical flux of eddy geopotential energy into the upper stratosphere of the N.H. (fig. 9). This flux was responsible for the minor warmings at 40 mb culminating on day 118, and 10 mb culminating on days 112 and 120. Further details of the energetics of this and other sudden warming-type events in the model are given by Trenberth (1973) and will not be considered further here.

The model has produced a change in activity in different waves; associated with the increased meridional heating gradient being set up by the onset of winter, similar to that found in dishpan experiments. While an increase in the static stability was precluded in the model, the increase in the intensity of the circulation was most noticeable, and it occurred suddenly and spontaneously.

Apparently this increase in the circulation intensity is a common feature of the observed circulation. Computations by Krueger et al. (1965), for October 1958–July 1963 showed the most pronounced change of this sort to occur in January 1963. At this time a large increase in baroclinic conversion terms produced a marked decrease in AZ while KE increased in the 800- to 500-mb layer. These changes were apparently the source of the vertically propagating energy that produced the major sudden stratospheric warming the following week (Finger and Teweles 1964, Miyakoda 1963). Teweles (1958), Finger and Teweles (1964), and Labitzke (1965) have also mentioned that warmings commence above a region of intense cyclonic activity.

Hence, it appears that sudden warmings may well be associated with an index cycle in the very long waves,

and this seems to be coupled with the annual heating cycle. The natural atmospheric variability probably affects the degree of coupling from year to year and, thus, may account for year to year differences observed in the stratospheric events.

In this integration, where there were no nonzonal effects, only a minor warming was produced. Clearly then, if we are to explain the hemispheric differences, we must also consider the coupling of this cycle with such things as nonzonal heating (land-sea heating contrast) and orography. This, as well as other possibilities, are considered by Trenberth (1973).

7. CONCLUDING REMARKS

We have described the development of an atmospheric model and some results of numerical time integrations. The model is a quasi-geostrophic spectral model but has many features not included in previous investigations. It is global, is extensive in the vertical with the highest level in the mesosphere at 0.05 mb (≈ 71 km), and has about 10-km resolution in the stratosphere. The model also incorporates an annual heating cycle, therefore, each hemisphere exhibits opposite seasonal circulations and trends.

While the model is clearly deficient in some ways, it appears suitable for the problem chosen for investigation and provides some insight into aspects of the upper atmospheric circulation that to date have been largely speculative.

The general features of the simulation for December and January were good in both hemispheres and at all levels. Although the effects of eddies on the model stratosphere were probably less than those that exist in the real atmosphere, the model indicated their importance, especially in winter, and showed them to be at least partly responsible for the observed temperature distribution in the mesosphere.

The presence of an annual heating cycle in the model, thereby including the effect of an increasing meridional

temperature gradient with the onset of winter, has allowed the atmosphere to change its baroclinic growth rate characteristics so that the longer waves may spontaneously and abruptly increase in activity. The increased poleward heat flux may thus cause the maximum tropospheric meridional temperature gradient to occur weeks prior to the maximum in the external heating field. A sudden increase in the vertical flux of eddy geopotential energy may also result, producing an adjustment in the stratospheric flow similar to a sudden warming.

APPENDIX

The spectral equations may be written as follows:

$$\begin{aligned} \frac{d\zeta_{m+n,j}^m}{dt} = & -i \sum_{l=0}^{\infty} \sum_{r=-\infty}^{\infty} \frac{\zeta_{r+s,j}^m \zeta_{|m-r|+l,j}^{m-r} L_{m+n,r,s,|m-r|+l}^{m,r,m-r}}{(|m-r|+l)(|m-r|+l+1)} \\ & + i b_n^m \zeta_{m+n,j}^m + (m+n+1) a_{n,j}^m (\omega_{m+n-1,j-1}^m - \omega_{m+n-1,j+1}^m) \\ & + (m+n) a_{n+1,j}^m (\omega_{m+n+1,j-1}^m - \omega_{m+n+1,j+1}^m) - g_{n,j}^m \zeta_{m+n,j}^m \\ & - k_j (\zeta_{m+n,j}^m - \zeta_{m+n,j-2}^m) - k'_j (\zeta_{m+n,j}^m - \zeta_{m+n,j+2}^m) \quad (22) \end{aligned}$$

where

$$\zeta_{n,-1}^m = 0,$$

$$\zeta_{n,19}^m = 0,$$

and

$$\omega_{n,18}^m = 0$$

for $m=0, n=1, 2, 3, 4, 5, 6$; and $m=2, 4, 6, n=1, 2, 3$; $j=1, 3, \dots, 17$.

$$\begin{aligned} \frac{d\theta_{m+n,j}^m}{dt} = & -i \sum_{l=0}^{\infty} \sum_{r=-\infty}^{\infty} \frac{\theta_{r+s,j}^m \zeta_{|m-r|+l,j}^{m-r} L_{m+n,r,s,|m-r|+l}^{m,r,m-r}}{(|m-r|+l)(|m-r|+l+1)} \\ & + \sigma_j \omega_{m+n,j}^m + h_j (\theta_{m+n,j}^m - \theta_{m+n,j}^m) - d_{n,j}^m \theta_{m+n,j}^m \quad (23) \end{aligned}$$

for $m=0, n=1, 2, 3, 4, 5, 6$; and $m=2, 4, 6, n=0, 1, 2$; $j=2, 4, \dots, 16$

and

$$\begin{aligned} \theta_{m+n,j}^m = & c_{n,j}^m (\zeta_{m+n-1,j-1}^m - \zeta_{m+n-1,j+1}^m) \\ & + c_{n+1,j}^m (\zeta_{m+n+1,j-1}^m - \zeta_{m+n+1,j+1}^m) \quad (24) \end{aligned}$$

for $m=0, n=1, 2, 3, 4, 5, 6$; and $m=2, 4, 6, n=0, 1, 2$; $j=2, 4, \dots, 16$,

where

$$\begin{aligned} a_{n,j}^m = & \frac{1}{m+n} \left\{ \frac{(2m+n)n}{[2(m+n)-1][2(m+1)+1]} \right\}^{1/2} \frac{2\Omega}{p_{j-1} - p_{j+1}}, \\ d_{n,j}^m = & \frac{(m+n)(m+n+1)}{a^2} E_j, \\ g_{n,j}^m = & \frac{(m+n+2)(m+n-1)}{a^2} E_j, \\ b_n^m = & \frac{2\Omega m}{(m+n+1)(m+n)}, \\ c_{n,j}^m = & \frac{a_{n,j}^m a^2 p_{00}}{(m+n) R p_j^{l-1}}, \end{aligned}$$

and

$$L_{n_1, n_2, n_3}^{m_1, m_2, m_3} = \frac{1}{2} \int_{-1}^{+1} P_{n_1}^{m_1}(\mu) \left[m_2 P_{n_2}^{m_2}(\mu) \frac{dP_{n_3}^{m_3}}{d\mu} - m_3 P_{n_3}^{m_3}(\mu) \frac{dP_{n_2}^{m_2}}{d\mu} \right] d\mu.$$

In eq (23) the $\zeta_{n,j}^m$ must be interpolated.

The nonlinear terms involving Jacobians and the effects of the earth's vorticity on the flow give rise to the interaction coefficients $L_{n_1, n_2, n_3}^{m_1, m_2, m_3}$, the $a_{n,j}^m$, and the $c_{n,j}^m$, as shown in Trenberth (1972). The method used for calculating the former is that given by Ellsaesser (1966).

ACKNOWLEDGMENTS

This work is part of my doctoral dissertation at Massachusetts Institute of Technology. My sincere thanks to Edward N. Lorenz for the advice and guidance he provided throughout. My stay at M.I.T. was made possible by a New Zealand Research Fellowship, and I am grateful to the New Zealand Meteorological Service for this. The calculations were performed at the MIT Computation Center and were supported by the Atmospheric Sciences Section, National Science Foundation, under NSF Grants GA-10276 and GA-28203X.

REFERENCES

- Bryan, Kirk, Jr., "A Numerical Investigation of Certain Features of the General Circulation," *Tellus*, Vol. 11, No. 2, Stockholm, Sweden, May 1959, pp. 163-174.
- Burger, Alewyn P., "Scale Considerations of Planetary Motions of the Atmosphere," *Tellus*, Vol. 10, No. 2, Stockholm, Sweden, May 1958, pp. 195-205.
- Byron-Scott, Roland, "A Stratospheric General Circulation Experiment Incorporating Diabatic Heating and Ozone Photochemistry," *Publication in Meteorology*, No. 87, Arctic Meteorology Research Group, McGill University, Montreal, Quebec, Apr. 1967, 201 pp.
- Charney, Jule G., "On the General Circulation of the Atmosphere," *Rossby Memorial Volume*, Bert Bolin (Editor), Rockefeller Institute Press, New York, N.Y., 1959, pp. 178-193.
- Charney, Jule G., "Integration of the Primitive and Balance Equations," *Proceedings of the International Symposium on Numerical Weather Prediction, Tokyo, Japan, November 1960*, Meteorological Society of Japan, Tokyo, Mar. 1962, pp. 131-152.
- Clapp, Philip F., "Normal Heat Sources and Sinks in the Lower Troposphere in Winter," *Monthly Weather Review*, Vol. 89, No. 5, May 1961, pp. 147-162.
- Clark, John H. E., "A Quasi-geostrophic Model of the Winter Stratospheric Circulation," *Monthly Weather Review*, Vol. 98, No. 6, June 1970, pp. 443-461.
- COESA, U.S. Committee on Extension to the Standard Atmosphere, *U.S. Standard Atmosphere Supplements, 1966*, U.S. Government Printing Office, Washington, D.C., 1966, 289 pp.
- Dickinson, Robert E., "On the Excitation and Propagation of Zonal Winds in an Atmosphere with Newtonian Cooling," *Journal of the Atmospheric Sciences*, Vol. 25, No. 2, Mar. 1968, pp. 269-279.
- Dopplick, Thomas G., "The Energetics of the Lower Stratosphere Including Radiative Effects," *Quarterly Journal of the Royal Meteorological Society*, Vol. 97, No. 412, London, England, Apr. 1971, pp. 209-237.
- Ellsaesser, Hugh, W., "Evaluation of Spectral Versus Grid Methods of Hemispheric Numerical Weather Prediction," *Journal of Applied Meteorology*, Vol. 5, No. 3, June 1966, pp. 246-262.
- Finger, Frederick, G., and Teweles, Sidney, "The Mid-winter 1963 Stratospheric Warming and Circulation Change," *Journal of Applied Meteorology*, Vol. 3, No. 1, Feb. 1964, pp. 1-15.
- Fultz, Dave, Long, Robert R., Owens, George V., Bohan, Walter, Kaylor, Robert, and Weil, Joyce, "Studies of Thermal Convection in a Rotating Cylinder with some Implications for Large-scale

- Atmospheric Motions," *Meteorological Monographs*, Vol. 4, No. 21, American Meteorological Society, Boston, Mass. Dec. 1959, 104 pp.
- Green, J. S. A., "A Problem in Baroclinic Stability," *Quarterly Journal of the Royal Meteorological Society*, Vol. 86, No. 368, London, England, Apr. 1960, pp. 237-251.
- Hines, C. O., "The Upper Atmosphere in Motion," *Quarterly Journal of the Royal Meteorological Society*, Vol. 89, No. 379, London, England, Jan. 1963, pp. 1-42.
- Holloway, J. Leith, Jr., and Manabe, Syukuro, "Simulation of Climate by a Global General Circulation Model: I. Hydrologic Cycle and Heat Balance," *Monthly Weather Review*, Vol. 99, No. 5, May 1971, pp. 335-370.
- Julian, Paul R., and Labitzke, Karin B., "A Study of Atmospheric Energetics during the January-February 1963 Stratospheric Warming," *Journal of the Atmospheric Sciences*, Vol. 22, No. 6, Nov. 1965, pp. 597-610.
- Katayama, A., "On the Heat Budget of the Troposphere over the Northern Hemisphere," Doctoral Dissertation, Tohoku University, Japan, 1964.
- Kidson, John W., and Newell, Reginald E., "Exchange of Atmospheric Angular Momentum between the Hemispheres," *Nature*, Vol. 221, No. 5178, Jan. 25, 1969, London, England, pp. 352-353.
- Kikuchi, Y., "Numerical Simulation of the Blocking Process," *Journal of the Meteorological Society of Japan*, Vol. 47, No. 1, Tokyo, Feb. 1969, pp. 29-53.
- Krueger, Arthur F., Winston, Jay S. and Haines, Donald A., "Computation of Atmospheric Energy and its Transformation for the Northern Hemisphere for a Recent Five-year Period," *Monthly Weather Review*, Vol. 93, No. 4, Apr. 1965, pp. 227-238.
- Kuhn, William R., and London, Julius, "Infrared Radiative Cooling in the Middle Atmosphere (30-110 km)," *Journal of the Atmospheric Sciences*, Vol. 26, No. 2, Mar. 1969, pp. 189-204; and corrigenda, Vol. 26, No. 3, p. 620.
- Labitzke, Karin B., "On the Mutual Relation between Stratosphere and Troposphere during Periods of Stratospheric Warmings in Winter," *Journal of Applied Meteorology*, Vol. 4, No. 1, Feb. 1965, pp. 91-99.
- Leovy, Conway, "Simple Models of Thermally Driven Mesospheric Circulation," *Journal of the Atmospheric Sciences*, Vol. 21, No. 4, July 1964, pp. 327-341.
- Lorenz, Edward N., "Maximum Simplification of the Dynamic Equations," *Tellus*, Vol. 12, No. 3, Stockholm, Sweden, Aug. 1960a, pp. 243-254.
- Lorenz, Edward N., "Energy and Numerical Weather Prediction," *Tellus*, Vol. 12, No. 4, Stockholm, Sweden 1960b, pp. 364-373.
- Lorenz, Edward N., "Simplified Dynamic Equations Applied to the Rotating-basin Experiments," *Journal of the Atmospheric Sciences*, Vol. 19, No. 1, Jan. 1962, pp. 39-51.
- Lorenz, Edward N., "The Mechanics of Vacillation," *Journal of the Atmospheric Sciences*, Vol. 20, No. 5, Sept. 1963, pp. 448-464.
- Lorenz, Edward N., "An N-cycle Time-differencing scheme for Stepwise Numerical Intergration," *Monthly Weather Review*, Vol. 99, No. 8, Aug. 1971, pp. 644-648.
- Manabe, Syukuro, and Hunt, Barrie G., "Experiments with a Stratospheric General Circulation Model: Radiative and Dynamic Aspects," *Monthly Weather Review*, Vol. 96, No. 8, Aug. 1968, pp. 477-502.
- Manabe, Syukuro, and Möller, Fritz, "On the Radiative Equilibrium and Heat Balance of the Atmosphere," *Monthly Weather Review*, Vol. 89, No. 12, Dec. 1961, pp. 503-532.
- Manabe, Syukuro, Smagorinsky, Joseph, Holloway, J. Leith Jr., and Stone, Hugh M., "Simulated Climatology of a General Circulation Model with a Hydrologic Cycle: III. Effects of Increased Horizontal Computational Resolution," *Monthly Weather Review*, Vol. 98, No. 3, Mar. 1970, pp. 175-212.
- Manabe, Syukuro, and Strickler, Robert F., "Thermal Equilibrium of the Atmosphere with a Convective Adjustment," *Journal of the Atmospheric Sciences*, Vol. 21, No. 4, July 1964, pp. 361-385.
- McIntyre, Michael E., "Baroclinic Instability of an Idealised Model of the Polar Night Jet," *Quarterly Journal of the Royal Meteorological Society*, Vol. 98, No. 415, London, England, Jan. 1972, pp. 165-174.
- Miyakoda, Kikuro, "Some Characteristic Features of Winter Circulations in the Troposphere and Lower Stratosphere," *Technical Report No. 14, N.S.F. (GP471)*, Department of Geophysical Sciences, University of Chicago, Ill., Dec. 1963, 93 pp.
- Miyakoda, Kikuro, Strickler, Robert F., and Hembree, G. D., "Numerical Simulation of the Breakdown of a Polar-night Vortex in the Stratosphere," *Journal of the Atmospheric Sciences*, Vol. 27, No. 1, Jan. 1970, pp. 139-154.
- Muench, H. Stuart, "On the Dynamics of the Wintertime Stratosphere Circulation," *Journal of the Atmospheric Sciences*, Vol. 22, No. 4, July 1965, pp. 349-360.
- Murgatroyd, R. J., "The Structure and Dynamics of the Stratosphere," *Proceedings of the Conference on the Global Circulation of the Atmosphere, August 25-29, 1969, London, England*, Royal Meteorological Society, The Salisbury Press, London, England, 1970, pp. 159-195.
- Murgatroyd, R. J., and Goody, Richard M., "Sources and Sinks of Energy from 30 to 90 km," *Quarterly Journal of the Royal Meteorological Society*, Vol. 84, No. 361, London, England, July 1958, pp. 225-234.
- Murray, F. W., "Dynamic Stability in the Stratosphere," *Journal of Geophysical Research*, Vol. 65, No. 10, Oct. 1960, pp. 3273-3305.
- Newell, Reginald E., "The Energy and Momentum Budget of the Atmosphere above the Tropopause," *Proceedings of the Sixth International Space Science Symposium, Mar del Plata, Argentina, May 11-19, 1965*, R. V. Garcia and T. F. Malone (Editors), Spartan Books, Washington, D.C., 1965, pp. 106-126.
- Newell, Reginald E., "The General Circulation of the Atmosphere above 60 km," *Meteorological Monographs*, Vol. 9, No. 31, American Meteorological Society, Boston, Massachusetts, 1968, pp. 98-113.
- Newell, Reginald E., Vincent, Dayton G., Dopplick, Thomas G., Ferruza, David, and Kidson, John W., "The Energy Balance of the Global Atmosphere," *Proceedings of the Conference on the Global Circulation of the Atmosphere, August 25-29, 1969, London, England*, Royal Meteorological Society, The Salisbury Press, London, England, 1970, pp. 42-90.
- Newton, Chester W., "Mountain Torques in the Global Angular Momentum Balance," *Journal of the Atmospheric Sciences*, Vol. 28, No. 4, May 1971, pp. 623-628.
- Oort, Abraham H., "On the Energetics of the Mean and Eddy Circulations in the Lower Stratosphere," *Tellus*, Vol. 16, No. 3, Stockholm, Sweden, Aug. 1964a, pp. 309-327.
- Oort, Abraham H., "On Estimates of the Atmospheric Energy Cycle," *Monthly Weather Review*, Vol. 92, No. 11, Nov. 1964b, pp. 483-493.
- Peng, Li, "A Simple Numerical Experiment Concerning the General Circulation in the Lower Stratosphere," *Pure and Applied Geophysics*, Basel, Switzerland, Vol. 61, No. 2, May 1965, pp. 191-218.
- Phillips, Norman A., "The General Circulation of the Atmosphere: A Numerical Experiment," *Quarterly Journal of the Royal Meteorological Society*, London, England, Vol. 82, No. 352, Apr. 1956, pp. 123-164.
- Reed, Richard J., Wolfe, John L. and Nishimoto, H., "A Spectral Analysis of the Energetics of the Stratospheric Sudden Warming of Early 1957," *Journal of the Atmospheric Sciences*, Vol. 20, No. 4, July 1963, pp. 256-275.
- Teweles, Sidney, "Anomalous Warming of the Stratosphere Over North America in Early 1957," *Monthly Weather Review*, Vol. 86, No. 10, Oct. 1958, pp. 377-396.
- Trenberth, Kevin E., "The Dynamic Coupling of the Stratosphere with the Troposphere and Sudden Stratospheric Warmings," *Doctoral Dissertation*, Department of Meteorology, Massachusetts Institute of Technology, Cambridge, Jan. 1972, 221 pp.
- Trenberth, Kevin E., "Dynamic Coupling of the Stratosphere With the Troposphere and Sudden Stratospheric Warmings," *Monthly Weather Review*, Vol. 101, No. 4, Apr. 1973, pp. 306-322.

[Received July 5, 1972; revised October 27, 1972]